University of Szeged
Faculty of Pharmacy
Department of Pharmaceutical Technology

APPLICATION OF NON-CONVENTIONAL METHODS IN THE PHYSICO-CHEMICAL PROCESSING OF PHARMACEUTICAL BIOPOLYMERS FOR THE AIM OF DRUG FORMULATION

PhD thesis

presented by

Anikó Szepes

Pharmacist

born on June 2th, 1979

Citizen of Hungary

Supervisors:

Prof. Dr. habil. Piroska Szabó-Révész
University of Szeged, Department of Pharmaceutical Technology

Prof. Dr.-Ing. habil. Joachim Ulrich
Martin-Luther-Universität Halle-Wittenberg
Zentrum für Ingenieurwissenschaften, Verfahrenstechnik/TVT

Szeged

2007

CONTENTS

LIST OF ORIGINAL PUBLICATIONS

This thesis is based on he following original papers, which are referred to in the text by the Roman numerals [**I – VII**].

I. **Szepes, A.**, Hasznos-Nezdei, M., Kovács, J., Funke, Z., Ulrich, J., Szabó-Révész, P., 2005. Microwave processing of natural biopolymers - studies on the properties of different starches, *International Journal of Pharmaceutics* 302, 166-171. **IF: 2.156**

II. **Szepes, A.**, Szabó-Révész, P., Erős, I., 2005. A mikrohullámú sütőtől a tudományig. [From the microwave oven to science] *Gyógyszerészet* 49 (4), 211-215.

III. **Szepes, A.**, Szabó-Révész, P., Mohnicke, M., Erős, I., 2005. Processing and storage effects on water sorption tendency and swelling characteristics of starches treated by microwave irradiation, *European Journal of Pharmaceutical Sciences* 25S1, S196-S198.

IV. **Szepes, A.**, Kovács, J., Szabó-Révész, P., 2006. Higanyos porozimetria és nitrogén adszorpció együttes alkalmazása tabletták pórusszerkezetének vizsgálatában [Use of mercury porosimetry assisted by nitrogen adsorption in the investigation of the pore structure of tablets], *Acta Pharmaceutica Hungarica* 76 (3), 23-29.

V. **Szepes, A.**, Ulrich, J., Farkas, Zs., Kovács, J., Szabó-Révész, P., 2007. Freeze-casting technique in the development of solid drug delivery systems, *Chemical Engineering and Processing* 46, 230-238. **IF: 1.159**

VI. **Szepes, A.**, Fehér, A., Szabó-Révész, P., Ulrich, J., Influence of freezing temperature on product parameters of solid dosage forms prepared via the freeze-casting technique, *Chemical Engineering and Technology*, accepted for publication. **IF: 0.678**

VII. **Szepes, A.**, Fiebig, A., Ulrich, J., Szabó-Révész, P., Structural study of α-lactose monohydrate subjected to microwave irradiation, *Journal of Thermal Analysis and Calorimetry*, accepted for publication. **IF: 1.425**

ABSTRACTS

VIII. **Szepes, A.**, Szabóné Révész, P., Funke, Z., Erős, I., 2003. Mikrohullámú kezelés befolyása különböző keményítő minták gyógyszetechnológiai alkalmazhatóságára, *Gyógyszerészet CPH XII, Különszám* 89.

IX. **Szepes, A.**, Szabó-Révész, P., Funke, Z., Ulrich, J., Hasznos-Nezdei, M., Erős, I., 2004. Influence of microwave treatment on pharmaceutical applicability of potato and maize starches, *International Meeting on Pharmaceutics, Biopharmaceutics and Pharmaceutical Technology, Nürnberg*, 669-670.

X. **Szepes, A.**, Szabó-Révész, P., Funke, Z., Ulrich, J., Hasznos-Nezdei, M., Erős, I., 2004. Application of microwave for the modification of physico-chemical properties of natural polymers in the pharmaceutical technology, *PharmaBioTec, Trieste.*

XI. **Szepes, A.**, Szabóné Révész, P., Hasznosné Nezdei, M., Farkas, Zs., Kovács, J., Erős, I., 2004. Mikrohullámú kezelés befolyása különböző keményítőminták fizikai-kémiai sajátságaira és gyógyszertechnológiai alkalmazhatóságára [Influence of microwave treatment on physico-chemical properties and pharmaceutical applicability of different starch samples], *Műszaki Kémiai Napok '04 Veszprém* , 225-227.
(ISBN 963 9495 37 9)

XII. **Szepes, A.**, Szabóné Révész, P., Erős, I., 2005. Mikrohullámmal kezelt keményítőminták vízadszorpciójának változása tárolás során [Moisture sorption behaviour of starch samples treated by microwave irradiation – effect of storage time], *Műszaki Kémiai Napok '05 Veszprém*, 21-22. (ISBN 963 9495 71 9)

XIII. **Szepes, A.**, Blümer, C., Mäder, K., Mohnicke, M., Ulrich, J., Kása jr., P., Szabó-Révész, P., 2005. Modification of the crystalline structure of natural biopolymers – Effects of isostatic ultrahigh pressure, *12th International Workshop on Industrial Crystallization (BIWIC), Halle/Saale*, 240-246. (ISBN 3-86010-797-6)

XIV. **Szepes, A.**, Szabó-Révész, P., Donchev, D., Ulrich, J., 2005. Freeze-casting in the development of porous drug-carrier formulations, *16th International Symposium on Industrial Crystallization (ISIC), Dresden*, VDI-Berichte 1901/2, 653-659. (ISBN 3-18-091901-9)

XV. **Szepes, A.,** Ulrich, J., Szabó-Révész, P., 2005. Formulation of a fast-dissolving delivery system containing theophylline using the freeze-casting technique, *1st BBBB Conference on Pharmaeutical Sciences, Siófok*, 227-229.

XVI. **Szepes, A.,** Blümer, C., Mäder, K., Mohnicke, M., Ulrich, J., Kása jr., P., Szabó-Révész, P., 2006. Isostatic ultrahigh pressure - a new tool for the modification of pharmaceutical excipients, *5th World Meeting on Pharmaceutics Biopharmaceutics and Pharmaceutical Technology*, Geneve.

XVII. **Szepes, A.**, Kása jr., P., Szabóné Révész, P., 2006. Izosztatikus ultranagy nyomás hatása keményítők szerkezetére és morfológiájára, *Congressus Pharmaceuticus Hungaricus XIII*, Budapest, p. 85, P-72.

XVIII. **Szepes, A.**, Makai, Zs., Blümer, C., Mäder, K., Ulrich, J., Szabó-Révész, P., 2006. Ultrahigh pressure in the processing of pharmaceutical biopolymers, *PolyPharma 2006, Halle/Saale,* P-28.

ABBREVIATIONS

d	[mm]	diameter
d_{mean}	[nm]	mean pore diameter
D (4V/F)	[nm]	mesopore diameter (4 Volume/Surface)
$D_v(d)$	[-]	volume pore size distribution
$D_{10\%}$	[µm]	particle size where 10% of the particles are finer
$D_{90\%}$	[[µm]	particle size where 90% of the particles are finer
f_1	[%]	difference factor
f_2	[-]	similarity factor
F	[-]	Fickian release fraction released due to the Fickian mechanism
h	[mm]	height
H	[N]	crushing strength
IUHP	[-]	isostatic ultrahigh pressure
k	[h^{-1}; $\%h^{-1}$]	rate constant of drug release
k_1	[$\%h^{-0.475}$]	kinetic constants associated with diffusional release
k_2	[$\%h^{-0.95}$]	kinetic constants associated with relaxational release
m	[-]	Fickian diffusion exponent
M_t	[%]	amount of drug released at time t
M_∞	[%]	initial drug amount
MS	[-]	maize starch
MS_{mw}	[-]	maize starch subjected to microwave irradiation
$MS_{130°C}$	[-]	maize starch subjected to conventional heating at 130 °C
MS-T	[-]	hydrogel containing maize starch and theophylline prepared via IUHP
MUR	[mg/g/day]	moisture uptake rate
n	[-]	diffusional exponent, sampling number
P	[MPa]	pressure
PS	[-]	potato starch
PS_{mw}	[-]	potato starch subjected to microwave irradiation
$PS_{130°C}$	[-]	potato starch subjected to conventional heating at 130 °C
PS-T	[-]	hydrogel containing potato starch and theophylline prepared via IUHP
R	[-]	release fraction released due to polymer relaxation

R^2	[-]	Pearson's coefficient (correlation coefficient)
R_j	[%]	percent dissolved of the reference at each time point j
S	[m^2/g]	total pore surface area
S_{BET}	[m^2/g]	specific surface area
SC	[-]	swelling capacity
SEM	[-]	scanning electron microscope
SP	[g/g]	swelling power
t_0	[min]	lag time of the drug dissolution
tan δ	[-]	dissipation factor
T_j	[%]	percent dissolved of the test products at each time point j
UHP	[-]	ultrahigh pressure
V	[cm^3; ml]	volume
$V_{p\ 1.7\text{-}300\ nm}$	[$m^3/g*10^4$]	mesopore volume
V_{tot}	[cm^3/g]	total intruded volume of mercury
W	[g]	weight
WRC	[-]	water retention capacity
WSI	[%]	water-soluble index
XRPD	[-]	X-ray powder diffraction
β	[-]	shape parameter of the dissolution curve
ε	[%]	porosity percentage
ε`	[-]	loss factor
ε``	[-]	dielectric constant
γ	[mN/m]	surface tension
γ^d	[mN/m]	disperse part of surface free energy
γ^p	[mN/m]	polar part of surface free energy
γ_{sl}	[mN/m]	interfacial tension of the solid and the liquid
γ_{sv}	[mN/m]	interfacial tension of the solid and the vapour
γ_{lv}	[mN/m]	interfacial tension of the liquid and the vapour
γ_{sv}^d	[mN/m]	disperse part of the interfacial tension of the solid and the liquid
γ_{lv}^d	[mN/m]	disperse part of the interfacial tension of the liquid and the vapour
γ_{sv}^p	[mN/m]	polar part of the interfacial tension of the solid and the vapour

γ_{lv}^{p}	[mN/m]	polar part of the interfacial tension of the liquid and the vapour
θ	[°]	contact angle
σ_x	[MPa]	tensile strength
ρ_h	[g/cm^3]	apparent particle density
τ	[min]	mean dissolution time, when 63.2% of M_∞ has been dissolved

1. INTRODUCTION

Considering the current requirements and guidelines concerning pharmaceutical research and manufacturing, the attention of pharmaceutical industry focused on processes which have been successfully utilized in other fields of the industry.

Microwave drying has been applied in food processing for decades. Several studies have been published evaluating the microwave drying process but sufficient data about the effects of electromagnetic irradiation on the structure and physico-chemical properties of frequently used pharmaceutical substances are not available. Since Process Analytical Technology (PAT) involves the design, analysis and control of manufacturing through timely measurements of critical quality of raw and in-process materials with the goal of ensuring final product quality, investigations of the possible changes in structure and physico-chemical properties resulted by microwave drying are of great practical importance.

Ultrahigh pressure treatment is known as a potential preservation technique in the food industry for almost over a century. This physical method offers a potential alternative for the sterilization and pasteurization of heat-sensitive substances and - considering the effect of high pressure on living cells and organisms – for the production of vaccines. Therefore, studies focusing on the effect of ultrahigh pressure on materials' properties and on its possible applications in pharmaceutical technology are essential for scientists and manufacturers alike.

In the practise of drug formulation, processing of heat- and pressure-sensitive materials is a great challenge for pharmaceutical technologists because pressure and friction accompanying the tableting process may result in modified physico-chemical properties of active pharmaceutical ingredients and excipients, which can lead to insufficient therapeutic efficiency and bioavailability.

Freeze-casting is a complex shape forming technique, which has been used for the production of porous ceramic bodies since the 1960s. This method is a specially designed freezing process based on the fluid-solid phase transition of water upon freezing and offers a promising new method for drug formulation from non-compressible pharmaceutical substances.

2. AIMS

This thesis is dealing with the utilization of the above-mentioned three non-conventional methods as possible alternatives for pharmaceutical processing and for drug design.

Starch is one of the most commonly used excipients in the formulation of solid dosage forms because it is a white, tasteless, odourless and relatively inert biopolymer. Starches, however,

possess poor flow properties and undergo elastic deformation during the tableting process. Therefore, starches are difficult to compress and compacts containing high amounts of this biopolymer indicate elastic recovery and capping.

Considering these properties, potato and maize starches were chosen as model substances in the experiments presented in this thesis.

- The morphological parameters and the structural changes of potato and maize starches subjected to microwave irradiation were investigated. The effects of volumetric heating and following storage on moisture content, sorption behaviour and swelling properties of the model substances were examined. The influence of the electromagnetic irradiation on the tensile strengths and surface free energies of compacts compressed from the processed polymers was also studied.
- The objective of the experiments connected to the freeze-casting technique was to develop a fast-dissolving solid dosage form containing theophylline as active ingredient possessing low flow properties and potato starch as a non-compressible diluent using the freeze-casting technique. The structure, the physical properties and mechanism of drug release from the freeze-casted units were investigated.
- The applicability of ultrahigh pressure for the aim of drug formulation was tested. Several studies reported that high pressure could evoke gelatinization of starch granules in excess water already at room temperature. In our experiments, aqueous suspensions of potato and maize starches containing theophylline as an active pharmaceutical ingredient were subjected to isostatic ultrahigh pressure. The changes in the structure and morphology of potato and maize starches were investigated. The release profile of theophylline from the pressurized samples was also studied.

3. THEORETICAL BACKGROUND

3.1. Starch: structure and functionality

Starch is a naturally-occurring ***biopolymer*** in which glucose is polymerized into amylose and amylopectin, forming a densely-packed, ***semicrystalline structure*** of particles with varying polymorphic types and degrees of crystallinity [1]. A widely accepted model of a starch granule involves alternating amorphous and crystalline lamellae, in which the two main components, amylose and amylopectin, are embedded (Fig. 1) [2].

X-ray powder diffraction studies have revealed that starches can be classified into A, B and C forms. The A pattern is mainly observed with cereal starches (e.g. maize starch), the B form is usually obtained from tuber starches (e.g. potato starch), while the C type

diffraction diagram, which has been demonstrated to be a mixture of the A- and B-type diagrams, is characteristic of most legume starches (Fig. 2) [3].

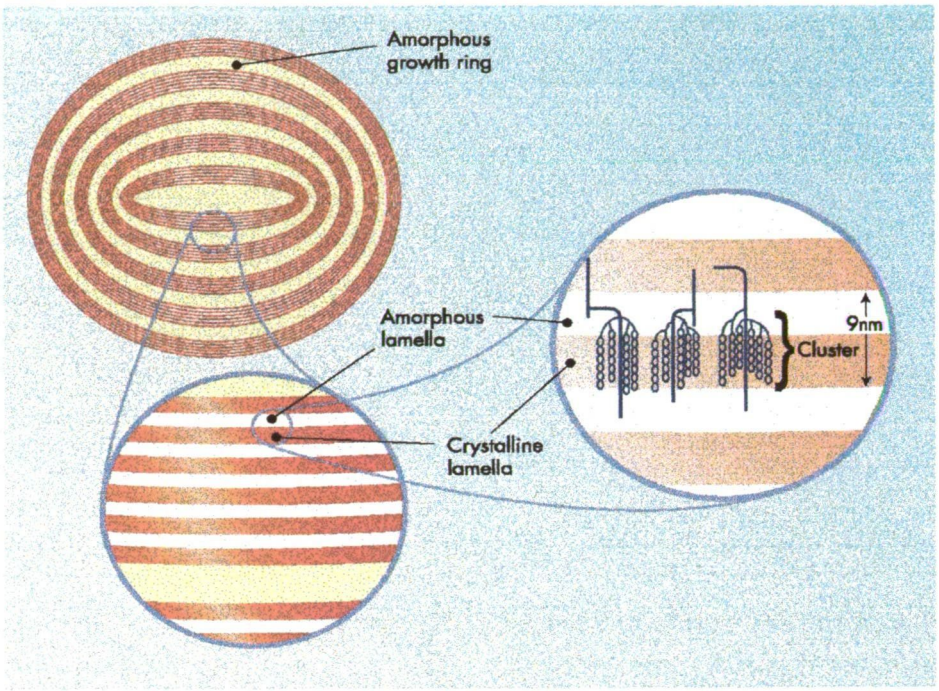

Figure 1 Schematic representation of the granule architecture of starches [4].

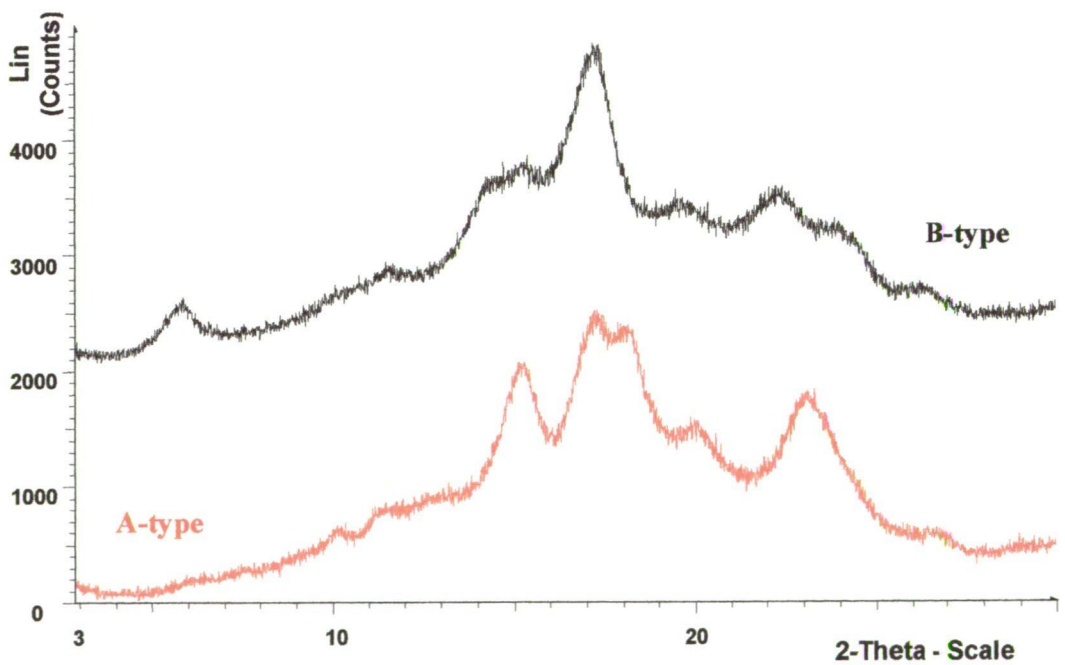

Figure 2 X-ray diffraction diagrams of A- and B-type starches [**III**].

The recent models for A- and B-type structures are based on parallel double-stranded helices, right-handed or left-handed and packed antiparallel or parallel in the unit cell. The left-handed form is energetically preferred to the right-handed form. In the ***A-structure***, these double helices are packed in a ***monoclinic unit cell*** (a = 2.124 nm, b = 1.172 nm, c = 1.069 nm, γ = 123.5 °) with eight water molecules per unit cell. In the ***B-type structure***, double helices are packed in a ***hexagonal unit cell*** (a = b = 1.85 nm, c = 1.04 nm) with 36 water molecules per unit cell (Fig.3).

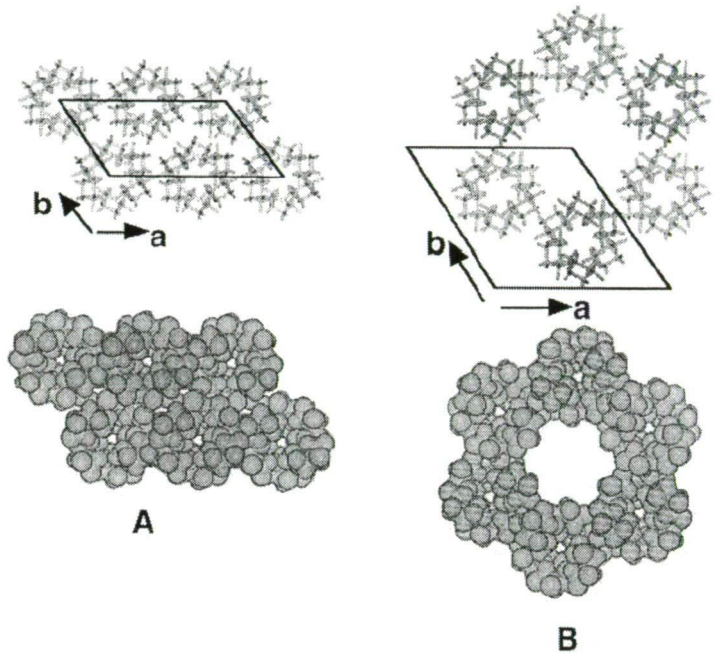

Figure 3 Crystalline packing of double helices in A-type (A) and B-type (B) amylose. Projection of the structure onto the (a, b) plane [3].

Starch is a fine white powder, which is an odourless, tasteless, non-toxic and non-irritant material. It is insoluble in alcohol, most solvents and cold water [5]. Various starch sources, starch modifications and starch derivatives provide a wide range of solids, which can be used in pharmaceutical applications. Starches and starch derivatives are primarily utilized in oral solid dosage formulations as binders, diluents and disintegrants [6].

The use of natural starch in technological processes causes a number of difficulties. In order to change the physico-chemical properties of starches so as to obtain the required features, different modifications are used. The simplest means of modification of starches is physical treatment, such as heating, the application of high pressure, mechanical methods and different forms of irradiations [7].

3.2. Microwaves

Microwaves belong to the portion of the electromagnetic spectrum with wavelengths from 1 mm to 1 m with corresponding frequencies between 300 MHz and 300 GHz (Fig. 4).

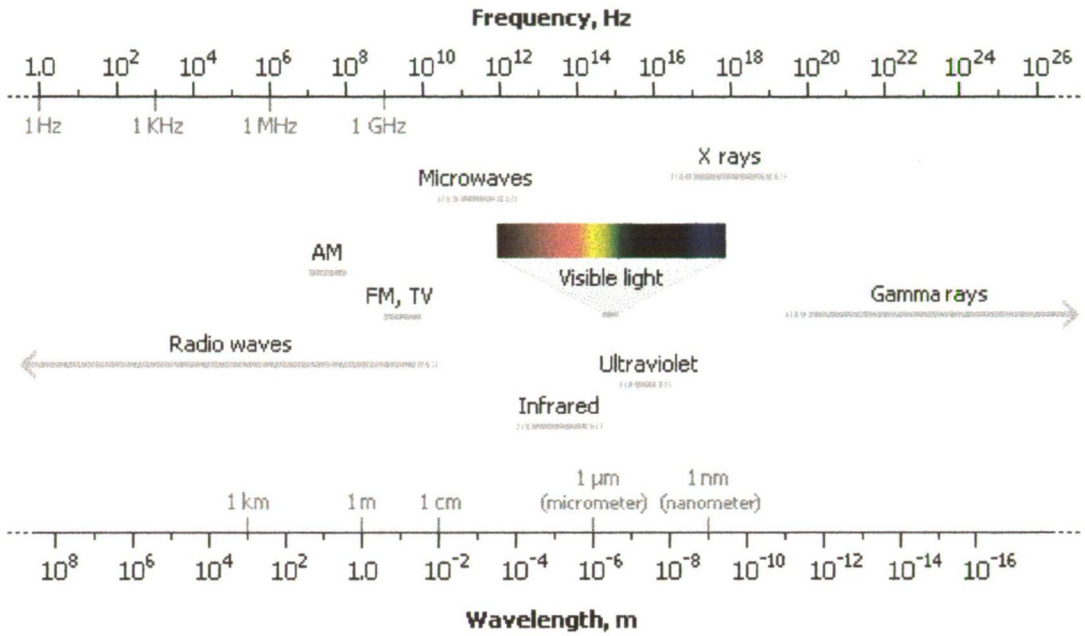

Figure 4 The electromagnetic spectrum [8].

The peculiarity of microwave heating is the energy transfer. In conventional heating processes, energy is transferred to the materials by convection, conduction and radiation phenomena through the external materials surface, in presence of thermal gradients. In contrast, microwave energy is delivered directly to materials through molecular interactions with electromagnetic field via conversations of electromagnetic energy into thermal energy [9]. Microwave energy is a non-ionizing radiation that causes molecular motion by migration of ions and rotation of dipoles, but does not cause changes in molecular structure. Typically, microwave energy is lost to the sample by two fundamental mechanisms: ionic conduction and dipole rotation. *Ionic conduction* is the conductive (i.e. electrophoretic) migration of dissolved ions in the electromagnetic field. *Dipole rotation* refers to the alignment, due to the electric field, of molecules in the sample that have permanent or induced dipole moments [10]. Dipole rotation is illustrated in Figure 5. As the electric field of the microwave energy increases, it aligns the polarized molecules (Fig. 5a). As the field decreases, thermally induced disorder is restored (Fig. 5b). When the field is removed, thermal agitation returns the molecules to disorder and thermal energy is released.

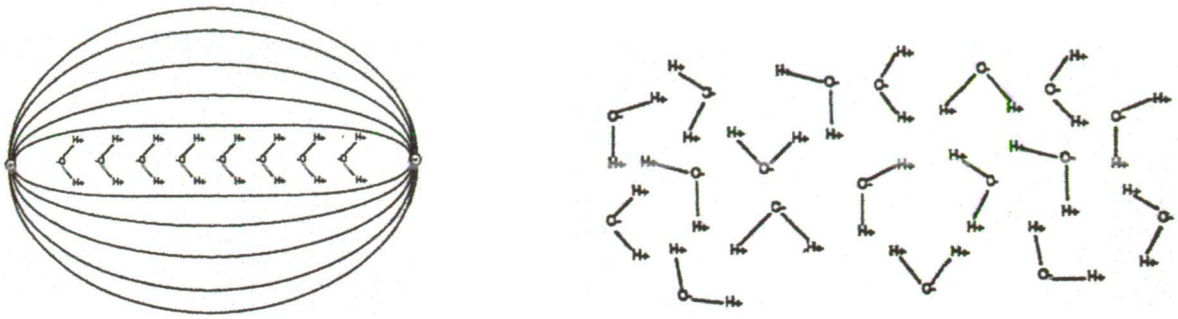

a. b.

Figure 5 Schematic of the molecular response to an electromagnetic field [10].
a., polarized molecules aligned with the poles of the electromagnetic field
b., thermally induced disorder as electromagnetic field is removed

Since microwaves can penetrate materials and deposit energy, heat can be generated throughout the volume of the material. The process is not dependent upon the thermal conductivity of the materials, and it is possible to achieve ***rapid and uniform heating*** of thick materials [10, 11] (Fig. 6).

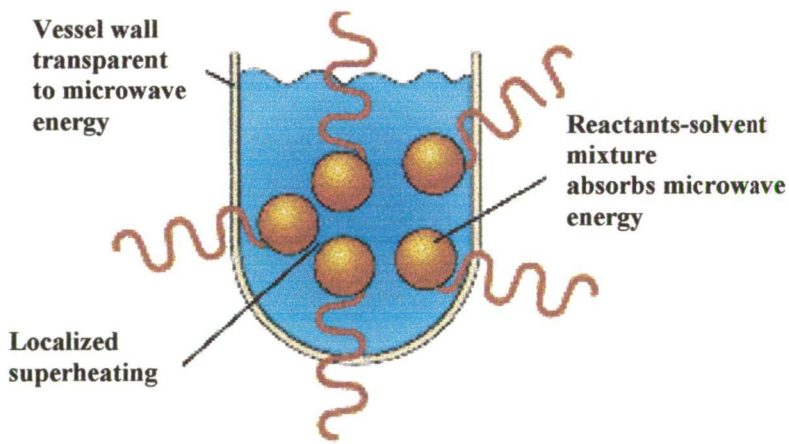

Figure 6 Schematic of sample heating by microwave energy [12].

In addition to ***volumetric heating***, microwaves can be utilized for ***selective heating*** of materials. The ability of a material to interact with electromagnetic energy is related to its complex permittivity and the dissipation factor (tan δ). The dissipation factor is a ratio of the sample's *loss factor* (ε `) to its *dielectric constant* (ε``) (Eq. 1) [10]. The dielectric constant is a measure of how much energy from an external electric field is stored in the material. The

loss factor accounts for the loss energy dissipative mechanisms in the material. Therefore, a material with a high loss factor is easily heated by microwave.

$$\tan \delta = \varepsilon' / \varepsilon'' \quad (1)$$

Generally, there are three qualitative ways in which a material may be categorized with respect to its interaction with the microwave field: *transparent* (low dielectric loss materials/insulators) – microwaves pass through with little, if any, attenuation; *opaque* (conductors) – microwave are reflected and do not penetrate; and *absorbing* (high dielectric loss materials) – absorb microwave energy to a certain degree based on the value of the dielectric loss factor (Fig. 7). It should be noted that water exhibits high losses in microwaves. Consequently, the absorption of matter is highly conditioned by its water content. Sample holders should be constructed from low-loss materials so that the microwaves will not be absorbed by the vessel but will pass through the vessel to the sample inside [10, 13]. Since metals reflect microwave irradiation, metals are forbidden to use for the construction of sample holders.

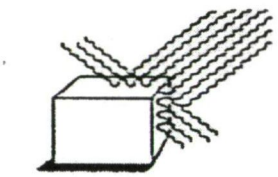

Opaque: metals

Transparent: ceramics, quartz, glass, Teflon, polystyrene

Absorbing: water, methanol, acetone

Figure 7 Interaction of materials with microwaves [10].

The primary benefits of microwave applications are reduction in manufacturing costs due to energy savings and shorter processing times, better production quality, synthesis of new materials and products as well as reduced hazards to the enviroment. These advantages have focused the attention on the use of electromagnetics in many fields such as materials processing, with special reference to polymers, ceramics and composites and enviromental remediation processes [14-21, **I**]. The use of microwave heating in organic synthesis reveals several features e.g. a reduction in thermal degradation, better selectivity, accelerated reaction rates etc. [22-28]. Medical applications are mainly related to hyperthermia therapy for the treatment of cancer [29, 30]. In pharmaceutical industry, microwave irradiation has been used because of its thermal effect in drying processes, for sterilisation of injections and infusions and in a frozen storage-microwave thawing system for intravenous infusions [31-42, **II, VII**].
In pharmaceutical technology, there is a steadily growing interest in the use of dielectric heating. Especially the combination of vacuum and microwave energy has received attention because of the possibility to dry moistened materials in a clean, fast and safe way with minimum handling and product loss [43-46].

3.3. Freeze-casting

Tablets account for a major proportion of the drug dosage forms administered today providing accurate drug dosage, good drug stability and the possibility of controlled drug delivery.
It is well known that direct compression is possible only for a limited number of substances. Many of the materials widely used for tablet formulation are difficult to compress because of their elastic compression behaviour and poor flow properties (e.g. theophylline, diclofenac-sodium, etc.). Furthermore, the tableting process is accompanied by friction and a rise in temperature. Accordingly, the compression of temperature-sensitive substances (e.g. ibuprofen and dimenhydrinate) and active agents tending to polymorphism (e.g. barbiturates, hydrocortison, phenylbutazone and carbamazepine) demands due foresight [47-50].
Freeze-casting is a ***complex shape-forming technique***, which has been used for the production of porous ceramic bodies since the 1960s [51-57]. The freeze-casting technique is a specially designed freezing process, which is based on the fluid-solid phase transition of water upon freezing. The essential steps of the process are shown in Figure 8 [58].

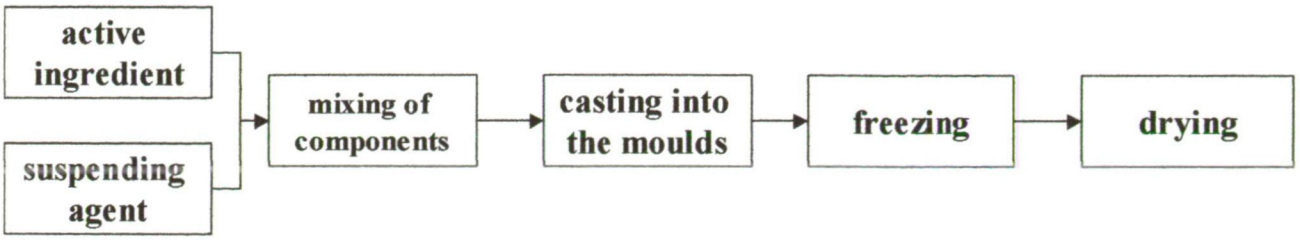

Figure 8 Flow chart of the freeze casting process [58].

When an aqueous suspension containing an active ingredient and further auxiliary materials (water-dispersible carrier materials, water-soluble binding materials, cryoprotectants, preservatives, flavouring agents, etc.) moulded into a form-giving tool undergoes freezing, the volume expansion due to the formation of ice from water results in the 'cold compression' of the suspended solid particles. After evaporation of the ice crystals, a porous solid body can be obtained [58-60] (Fig. 9). The open pores are the negative image of the former ice crystals.

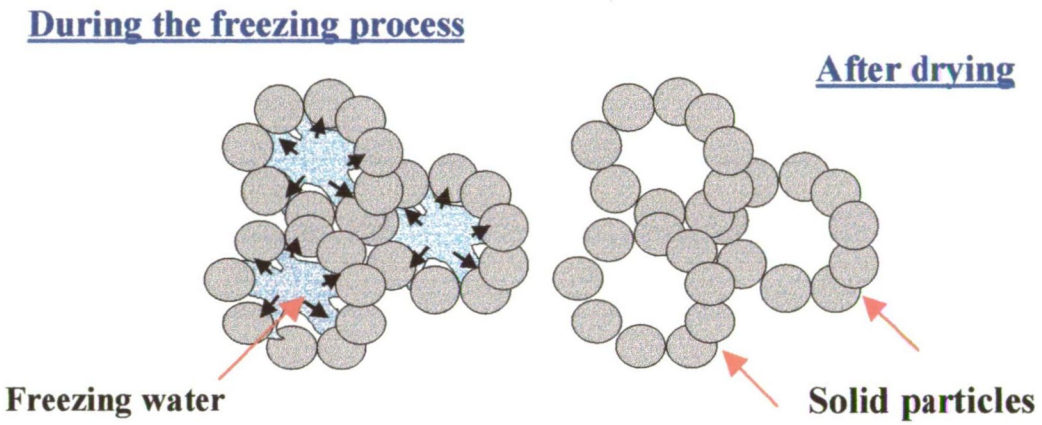

Figure 9 Formation of the pores [58].

The process was carried out by using an experimental setup shown in Chapter 4.1. (see Fig. 11).

During freezing, the aqueous suspension is only in contact with the cooling surface at the bottom, the upper surface is open to ambient conditions. Therefore, the temperature gradients created encourage the ice crystals to grow only in the vertical direction resulting in dendritic pore networks. As the freezing front proceeds from the cooling surface to the inferior of the suspension, the temperature gradient is the factor that effects the pore structure of the final

product. The regulation of heat transfer and the variation of the composition results in different pore structures, sizes and porosities.

The frozen units may be dried either by freeze-drying or the dispersing agent can be removed under conditions whereby the solvent is evaporated from the solid through the liquid phase to a gas. This may be achieved by vacuum drying or by forced air-drying, which is carried out at a temperature range of 15-30 °C for 1 to 6 days.

Consequently, the rise in temperature during tableting can be avoided by application of the freeze-casting technique. This process permits the drug-carrier formulation with the non-compressible substances mentioned above. A further advantage of this method is that the channel-like structure of the freeze-casted solid bodies resulting from the ice-crystal growth allows a better matrix-solvent interaction and hence faster drug dissolution, enhanced bioavailability and an improved therapeutic effect of the active ingredient [61]. Furthermore, freeze-casting can be regarded as an environmentally friendly, so-called ***green technology***, because the application of any organic solvents can be avoided.

3.4. Isostatic ultrahigh pressure

Ultrahigh pressure (UHP) treatment is known as a potential preservation technique for almost over a century, since Hite demonstrated in 1899 that microbial spoilage of milk could be delayed by application of high pressure. High pressure has been applied for many years for production of ceramics, composite materials, carbon graphite and plastics. UHP causes inactivation of microorganisms and enzymes while leaving small molecules, such as vitamins intact. Emulsions, which are sensitive to heat, can be pressure-treated without affecting the stability of the emulsion. Therefore, high pressure technology can be defined as ***mild technology*** [62-67].

Two principles underlie the effect of high pressure. Firstly, the principle of Le Chatelier according to which any phenomenon (phase transition, chemical reaction, change in molecular configuration) accompanied by a decrease in volume will be enhanced by pressure. As a result, pressure favours the crystalline state.

Secondly, pressure is instantaneously and uniformly transmitted independent of the size and the geometry of the materials. This is known as ***isostatic pressure***.

1 bar corresponds to the pressure exerted by a water column with a height of 10 metres. ***Ultrahigh pressure*** begins at 1000 bar (1000 bar = 100 MPa) [68].

Biopolymers, such as starches and proteins, show changes of their native structure under high hydrostatic pressure analogous to the changes occurring at high temperatures. The

effect of pressure on proteins and enzymes is related to reversible or irreversible changes of the native structure [69-71]. Temperature and/or chemical induced protein denaturation often unfold the complete protein irreversibly because of covalent bond breaking and/or aggregation of the molecule. In contrast, high pressure can leave parts of the molecule unchanged, indicating that the denaturation mechanisms are substantially different. In aqueous solution, pressure affects mainly the tertiary and quaternary structure of proteins. Covalent bonds are rarely affected by high pressure and even α–helix or β–sheet structures appear to be almost incompressible. Since solvent water has to be considered as an integral part of dissolved enzymes, the hydration patterns of side chains strongly affect the stability of enzymes and their catalytic reactions. In contrast to temperature which destabilizes the protein molecule by transferring non-polar hydrocarbons from the hydrophobic core towards the water, pressure denaturation is initiated by forcing water into the interior of the protein matrix.

Several authors reported that high pressure could evoke gelatinization of starch granules in starch-water suspensions already at room temperature, although the degradation of granules happens in a different manner (Fig. 10) [72-78].

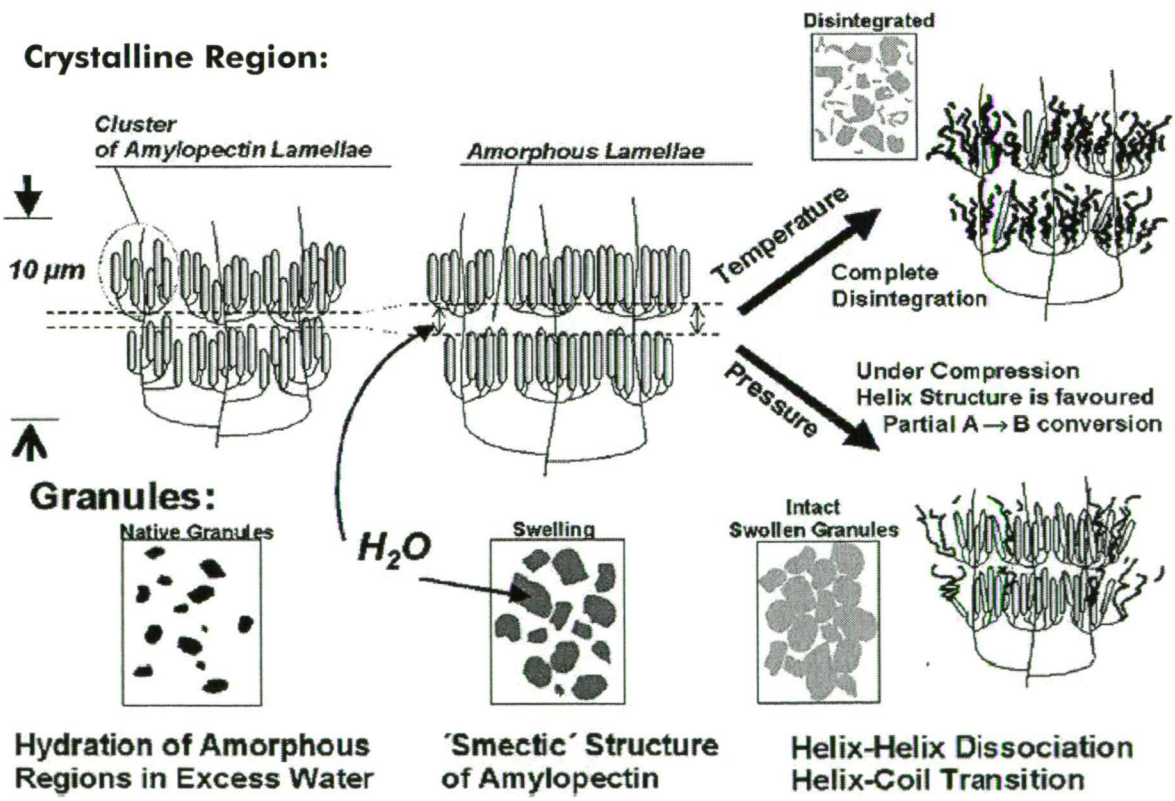

Figure 10 Scheme of starch gelatinization [69].

Gelatinization is generally considered to be a multi-stage process. After the swelling of the amorphous domains, the growth ring structure of the granule starts to disintegrate and the crystalline regions undergo melting simultaneously with a progressively increasing hydration. The smectic crystalline structure is decomposed by helix-helix dissociation followed by helix coil transition when the gelatinization temperature is exceeded. Increasing particle size and re-association of solubilized amylose are producing an increase in viscosity and gel formation. However, different from heat gelatinization, the pressurized starch granules remain intact or just partly disintegrated and the solubilization of amylose is rather poor. The disintegration of the macromolecule is incomplete since the pressure stabilization of van der Waals and hydrogen bonds favours the helix conformation. Even crystalline conversion from A- to B-isomorph under pressure has been reported (Fig. 10).

4. MATERIALS AND METHODS

4.1. Physical treatments

- ***Microwave processing***

Microwave processing of the starch samples was achieved in two different ways:

  - by **microwave irradiation** for *15 minutes* in a Sharp R4P58 (*450 W*) microwave oven (**PS_{mw}** and **MS_{mw}**),
  - by **conventional heating** at *130 °C for 2 hours* (**$PS_{130°C}$** and **$MS_{130°C}$**) in a drying oven without air flow [7, 79, 80].

In both cases, 100.0 g powder was modified. The initial and the processed samples were stored in well-closed vessels at room temperature (20±2 °C; 45±5% RH) until the beginning of the measurements. The starch samples used for the examination of sorption behaviour and swelling properties were stored for 6 months (25±2 °C; 50±5% RH).

- ***Freeze-casting procedure***

The binary powder mixture applied for the preparation of the suspensions was prepared by mixing 93% (w/w) potato starch (23.72 – 75.28 μm) (Amylum solani, Hungaropharma, Budapest, Hungary) and 7% (w/w) anhydrous theophylline (29.19 - 1023.64 μm) (Theophyllinum, Hungaropharma, Budapest, Hungary) in a Turbula mixer (Willy A. Bachofen, Maschinenfabrik, Basel, Switzerland) at 50 rpm during 5 minutes. The moisture content of the powder mixture was 5.57±0.20%. The compositions and the amount of the suspending agents are shown in Table 1.

Table 1 Compositions of the suspensions applied for the freeze-casting process.

Sample	Suspending agent	Amount of the suspending agent [% (w/w)]	Viscosity of the suspensions [Pas]	Gelatinization temperature of the suspensions [°C]
Sample 1	Distilled water	48	1.41±0.12	58.47
Sample 2	9% aqueous solution of citric acid	54	0.72±0.03	57.85
Sample 3	20% aqueous solution of saccharose	57	1.52±0.15	57.70

The aqueous suspensions were mixed and poured into cylindrical plastic forms 13 mm in diameter. The moulding forms were placed on a cooling cell connected with a thermostat ($t_{freezing}$ = -20 °C). The suspension was only in contact with the cooling surface at the bottom. The top of the moulding forms was open to the atmosphere at room temperature (Fig. 11). The resulting temperature gradient enforced vertical ice-crystal growth [58-60]. After freezing, the ice crystals were evaporated by forced-air drying, in an air-drier for 24 h (t_{drying} = +30 °C).

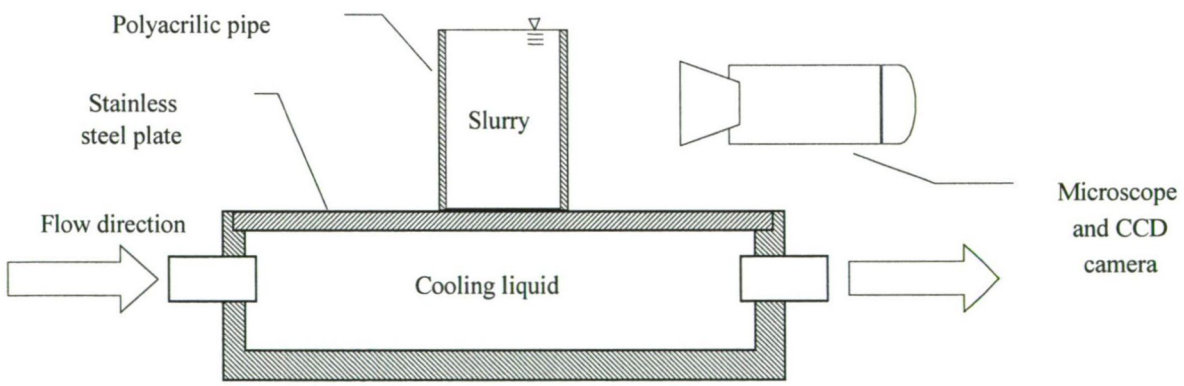

Figure 11 Experimental setup used for the freeze-casting process [58].

- ***Isostatic ultrahigh pressure (IUHP) treatment***

For the preformulation studies, approximately 4.0 g samples of starch-water suspensions (potato starch: 30% (w/w), maize starch: 20% (w/w)) were pressurized in a high-pressure device equipped with a temperature control (Mini Foodlab, Stansted Fluid Power Ltd.,

Stansted, Essex, UK). The samples were pressure-treated at 300 or 700 MPa for 5 or 20 min (Table 2).

Table 2 Conditions of processing of starch samples.

Samples	Starch	Applied pressure [MPa]	Duration of pressure treatment [min]
PS_{300-5}	PS	300	5
PS_{700-5}	PS	700	5
PS_{700-20}	PS	700	20
MS_{300-5}	MS	300	5
MS_{700-5}	MS	700	5
MS_{700-20}	MS	700	20

On the basis of the preformulation studies, pressurization at 700 MPa for 5 minutes was chosen to prepare gel samples containing theophylline as an active pharmaceutical ingredient. The profile of theophylline release was investigated from hydrogels containing 8% (w/w) theophylline, 32% (w/w) starch and 60% (w/w) water, produced via IUHP treatment at 700 MPa for 5 minutes (**PS-T; MS-T**).

4.2. Measuring techniques

- ***Moisture content***

Moisture content was determined by using the HR73 Halogen Moisture Analyzer (Mettler-Toledo GmbH, Greifensee, Switzerland). Approximately 4 g material was heated at 60 °C and the change in mass was recorded with a precision of 0.1 mg. Each sample was measured three times under the following conditions: *weight loss per unit of time*: 3-factory setting (Drying is automatically ended as soon as the mean weight loss (Δg in mg) per unit of time (Δt in seconds) drops below 50 seconds.); *drying program*: standard drying (The sample is heated to the drying temperature and held constant at this temperature.); *display mode*: moisture content (The moisture content of the sample is displayed as a percentage of the wet weight.).

- ***Particle size distribution***

The particle size and its distribution for all samples were measured by laser diffraction (Malvern Mastersizer 2000, Malvern Ltd., Worcestershire, UK). For the measurements, the

samples were dispersed in air. The particle size was determined in the range of 0.02-2000 μm. The measurements were repeated three times.

- ***Microscopic investigation***

The morphological investigations (particle form and particle surface) of the starches were carried out by a ***scanning electron microscope (SEM)*** (Philips XL 30 ESEM). Particles for scanning microscopy examination were mounted and coated with gold in a sputter coater (Polaron Equipment, Greenhill, UK). The air pressure was 1.3-13.0 mPa. The surfaces of the particles were treated with gold for 60 s (coating thickness: 18 nm).

The morphology of the starch suspensions and gels generated by *IUHP* was analysed with a ***stereomicroscope*** (Zeiss KL 1500 LCD, Jena, Germany) after drying at room temperature. The texture of the pressurized samples was investigated with a ***SEM*** (Hitachi 2400 S, Hitachi Scientific Instruments Ltd., Tokyo, Japan). A polaron sputter coating apparatus (Bio-Rad SC502, VG Microtech Uckfield, UK) was applied to create electric conductivity on the surface of the samples.

- ***Micromorphological studies***

The ***specific surface areas*** and ***micropore volumes*** of the samples were determined with Micromeritics ASAP 2000 equipment (Instrument Corp., Norcross, GA, USA) from the data of nitrogen adsorption and desorption isotherms at the boiling point of liquid nitrogen under atmospheric pressure (–196 °C). The specific surface was calculated in the validity range of the BET (Brunauer, Emmett, Teller) isotherm from the slope and intercept of a line characterized by five measuring points [81]. The samples (1.5-2.0 g) were degassed at 60 °C in a vacuum up to 1 Pa absolute pressure. After degassing, the samples were weighed again and the morphological parameters were calculated for the "surface-cleaned" masses of the samples. The micropore volumes were calculated via the BJH (Barrett, Joyner, Halenda) method [82]. The investigations were made in triplicate.

Porosity parameters, total pore volume, total pore surface area and pore volume size distributions were determined with a high-pressure mercury porosimeter (High Pressure Mercury Porosimeter Porosimetro 70, Carlo Erba Apparecchi Stientifici Ltd., Italy). Low pressure measurements between 0.01 and 100 kPa were performed to measure pores with a diameter between 1.9 and 58 μm. The pressures used for high-pressure measurements varied from 0.1 to 200 MPa, which correspond to pore diameters in the range of 7.5 nm – 15 μm. Porosimeter tests were carried out in triplicate.

Volume pore size distribution, $D_v(d)$, is defined as the pore volume per unit interval of pore radius by Eq. (2) [83-85]:

$$D_v(d) = \frac{P}{d} \times \frac{dV}{dP} \quad (2)$$

where P is the pressure, d is the pore diameter and V is the intruded volume of mercury.

Total pore surface area (S) was calculated according to Eq. (3):

$$S = \frac{1}{\gamma |\cos\theta|} \int_0^{Vtot} P dV \quad (3)$$

where P is the pressure, V is the intruded volume of mercury, γ is the surface tension, θ is the contact angle of mercury and V_{tot} is the total intruded volume of mercury [84, 85]. The surface tension and the contact angle values used in calculations for mercury were 480 mN/m and 141.3°.

The ***mean pore diameter*** (d_{mean}) was calculated via Eq. (4):

$$d_{mean} = 4 \times \frac{V_{tot}}{S} \quad (4)$$

The ***porosity percentage*** (ε) based on the porosimeter analysis was calculated by the following equation (Eq. (5)) [83]:

$$\varepsilon = \left(\frac{V_{tot}}{V_{tot} \times \frac{1}{\rho_h}} \right) \times 100 \ (\%) \quad (5)$$

where ρ_h is the apparent particle density of the powder mixtures used for the preparation of the samples and the tablets determined by a helium pycnometer (Quantachrome SPY-2 Stereopycnometer, Quantachrome Corp., Syosset, New York, USA). The pycnometric density was calculated from the mass and the pycnometric volume. Results are averages of three parallel determinations.

- ***X-ray powder diffraction (XRPD)***

The X-ray diffraction profiles were taken using a D4 Endeavour Diffractometer (Bruker AXS GmbH, Karlsruhe, Germany). The measurement conditions were as follows: radiation source: CuKα, angle of diffraction scanned: from 1° to 30°, step size: 0.01°, step time: 8 s.

- ***Preparation and investigation of the compacts***

Compacts were compressed with an instrumented eccentric tableting machine (Korsch EK0, Berlin, Germany). The punch holders were equipped with flat plane-parallel punches 10 mm in diameter. The rate of compression was 30 tablets/min at an air temperature of 24 °C and an air relative humidity of 45%.

Compacts used in the investigations connected to microwave processing were compressed using a binary powder mixture, which was prepared by mixing 80% (w/w) microcrystalline cellulose (Avicel® PH 101, FMC Corp., Philadelphia, USA) (25.30 – 93.60 μm) and 20% (w/w) starch in a Turbula mixer (Willy A. Bachofen, Maschinenfabrik, Basel, Switzerland) at 50 rpm during 2 minutes. The mean compression force was 2±0.5 kN (for measurements of tensile strength) and 20±1 kN (for determination of contact angles).

The properties of the freeze-casted samples were compared with those of tablets compressed using three different compression forces (compression force: Tablet/20 kN = 20±2 kN; Tablet/10 kN = 10±2 kN; Tablet/5 kN = 5±1 kN).

The composition of these tablets was as follows: anhydrous theophylline 100 g, potato starch 40 g, magnesium stearate 1 g and Avicel PH 101 159 g for 1000 tablets. The components were mixed for 5 minutes with a Turbula mixer (Willy A. Bachofen, Maschinenfabrik, Basel, Switzerland).

The crushing strengths of the tablets (σ_x) were measured with the Heberlein equipment (Heberlein and Co. AG, Zürich, Switzerland), while tensile strengths were calculated from these strength data and the geometrical parameters of the tablets (Mitutoyo OP 1-HS, Japan) via the following equation [86] (Eq. (6)):

$$\sigma_x = \frac{2H}{\pi \cdot d \cdot h} \tag{6}$$

where H is the crushing strength [N], d is the diameter [mm] and h is the height of the tablets [mm].

- ***Contact angle and surface free energy***

Surface free energies were determined by contact angle measurements with polar (bidistilled water) and non-polar (diiodomethane, Merck KGaA, Darmstadt, Germany) liquids, using the OCA 20 Optical Contact Angle Measuring System (Dataphysics, Filderstadt, Germany) with the sessile drop method. Surface free energies were calculated via the equation of Owens-Wendt [87] (Eq. (7)):

$$\gamma_{sl} = \gamma_{sv} + \gamma_{lv} - 2\sqrt{\gamma_{sv}^{d}\gamma_{lv}^{d}} - 2\sqrt{\gamma_{sv}^{p}\gamma_{lv}^{p}} \tag{7}$$

Where: γ_{sl} = interfacial tension of the solid and the liquid [mN/m], γ_{sv} = interfacial tension of the solid and the vapour [mN/m], γ_{lv} = interfacial tension of the liquid and the vapour

[mN/m], γ_{sv}^{d} = disperse part of the interfacial tension of the solid and the liquid [mN/m], γ_{lv}^{d} = disperse part of the interfacial tension of the liquid and the vapour [mN/m], γ_{sv}^{p} = polar part of the interfacial tension of the solid and the vapour [mN/m], and γ_{lv}^{p} = polar part of the interfacial tension of the liquid and the vapour [mN/m].

- ***Water retention capacity (WRC)***

100 ml of freshly prepared suspension (20% (w/w)) was centrifuged for 30 min at 4500 rpm (High-speed Refrigerated Centrifuge Cenrikon T-42, Kontron Instruments). The supernatant was removed by suction and the residue was weighed (W_1), and then dried at 60 °C to constant mass (W_2) [88, 89]. The measurements were made in triplicate.

$$WRC = W_1/W_2 \tag{8}$$

- ***Swelling capacity (SC)***

A modification of the method described by Bowen and Vadino was used [88, 90].
5 g of starch was poured into a 25 ml volumetric cylinder and the bulk volume was measured (V_1). 10 ml of deionized water was added and the suspension was well shaken for 5 min. Water was added up to 25 ml. The samples were allowed to stand for 24 h and the sedimentation volume was read off (V_2). Three parallel measurements were carried out.

$$SC = V_2/V_1 \tag{9}$$

- ***Swelling power (SP)***

SP was determined in triplicate on 0.1 g of starch by a modification of the method of Tsai et al. [91, 92]. Starch was weighed into a centrifuge tube with a coated screw cap, and 10 ml distilled water was added. The tube was heated at 80 °C in a shaking water bath for 1 h. The tube was cooled to room temperature in an iced water bath and centrifuged at 8800 rpm for 20 min (High-speed Refrigerated Centrifuge Cenrikon T-42, Kontron Instruments). The supernatant was poured out from the tube. Only the material adhering to the wall of the centrifuge tube was regarded as sediment and weighed (W_S). The supernatant was dried to constant mass (W_1) in an air oven at 100 °C. The water-soluble index (WSI) and SP were calculated as follows:

$$WSI = (W_1/0.1) * 100 \quad (\%) \tag{10}$$

$$SP = W_S / [0.1 * (100\text{-}WSI)] \quad (g/g) \tag{11}$$

- ***Rheological characterization of the suspensions used in the freeze-casting process***

Rheology of the aqueous suspensions was performed by using a Physica MCR 101 Rheometer (Anton Paar GmbH, Graz, Austria).

All measurements were carried out with a stainless steel coaxial cylinder measuring system at 25±0.1 °C with a shear rate of 0.1 – 100 s^{-1} during an interval of 120 seconds. 30 data points were recorded for each rheogram. Five replicates were performed. Viscosity was obtained from the up-curve of rotational measurements at a shear rate of 100 s^{-1}. In order to characterize the gelatinization behaviour of the starch suspensions, samples were heated to 85°C (1°C/min). Gelatinization temperature was obtained from the decrease of the loss tangent curve, which is an indicative of the gelation process [93].

- ***Characterization of drug dissolution from the freeze-casted samples***

The dissolution profiles of the solid units were investigated according to the European Pharmacopoea with a paddle method (Pharma Test PTW II, Pharma Test GmbH, Germany), using a UV-VIS spectrophotometer (Unicam Heλios-α, Spectronic Unicam, UK) at 269 nm. The dissolution medium was 900 ml artificial gastric juice (pH=1.2±0.1) and its temperature was 37±0.5 °C. The paddle speed was 100 rpm. The measurements were made in triplicate.

- **In vitro drug diffusion study of the hydrogels prepared by IUHP (diffusion cell method)**

In vitro drug release studies were performed by means of a vertical diffusion cell method (Hanson SR8-Plus™ Dissolution Test Station, Hanson Research Corporation, Chatsworth CA, USA). 0.50 g of sample (PS-T; MS-T) was placed as a donor phase on the Porafil membrane filter with a pore diameter of 0.45 μm. The effective diffusion surface area was 7.069 cm^2. 70 ml buffer (pH = 5.43) was used as acceptor phase to ensure sink conditions. The pH of the applied buffer approaches the natural pH value of human skin. Therefore, this kind of buffer is usually used as dissolution medium for the investigation of transdermal drug delivery. The membranes were soaked in buffer for 15 min before starting the tests. Investigations were performed at 37 °C for 6 h. The quantitative determination of theophylline was carried out with a UV-VIS spectrophotometer (Unicam Heλios-α, Spectronic Unicam, UK) at a wavelength of λ = 271 nm. In order to compare dissolution profiles, an aqueous suspension of theophylline was used as a reference (T). Three parallel measurements were carried out.

- ***Characterization of the mechanism of drug release***

The following mathematical models were evaluated considering the dissolution profiles of the samples [94-96].

Zero-order model

The drug release from the dosage form follows a 'steady-state release' running at a constant rate:

$$\frac{M_t}{M_\infty} = kt \tag{12}$$

where M_t is the amount of drug released at time t, M_∞ is the initial drug amount and k is the rate constant of drug release.

First-order model

The drug activity within the reservoir is assumed to decline exponentially and the release rate is proportional to the residual activity:

$$\frac{M_t}{M_\infty} = 1 - \exp(-kt) \tag{13}$$

Higuchi square root time model

The most widely used model to describe drug release from matrices, derived from Higuchi for a planar matrix, however it is applicable for systems of different shapes too:

$$\frac{M_t}{M_\infty} = kt^{1/2} \tag{14}$$

Weibull distribution

A general empirical equation described by Weibull was adapted to the dissolution/release process. This equation can be successfully applied to almost all kinds of dissolution curves and is commonly used in these studies [97].

$$\frac{M_t}{M_\infty} = 1 - \exp\left\{-\left[(t - t_0)/\tau\right]^\beta\right\} \tag{15}$$

where t_0 is the lag time of the drug dissolution, τ is the mean dissolution time, when 63.2% of M_∞ has been released and β is a shape parameter of the dissolution curve.

Hixson-Crowell model

The model describes the release from systems showing dissolution rate limitation and does not dramatically change in shape as release proceeds. When this model is used, it is assumed that the release rate is limited by the drug particle dissolution rate and not by the diffusion that might occur through the polymeric matrix.

$$\left(1 - \frac{M_t}{M_\infty}\right)^{1/3} = 1 - kt \tag{16}$$

Korsmeyer-Peppas model

Ritger and Peppas proposed an equation to describe drug release kinetics from drug delivery systems controlled by swelling [98-101]. The equation is based on a power law dependence of the fraction released on time and has the following form:

$$\frac{M_t}{M_\infty} = kt^n \tag{17}$$

where n is the diffusional exponent, which can range from 0.43 to 1 depending on the release mechanism and the shape of the drug delivery device. Based on the value of the diffusional exponent, the drug transport in slab geometry is classified either as Fickian diffusion (n = 0.5), non-Fickian or anomalous transport (0.5 < n < 1), or Case II transport (n = 1), where the dominant mechanism for drug transport is due to polymer relaxation during gel swelling. Anomalous transport occurs due to a coupling of Fickian diffusion and polymer relaxation.

In the anomalous processes of drug release, Fickian diffusion through the hydrated layers of the matrix and polymer chain relaxation/erosion are both involved [99, 100]. The contribution of these two mechanisms to the overall release are considered to be additive. The empirical model of Peppas and Sahlin describes these phenomena [101]:

$$\frac{M_t}{M_\infty} = k_1 t^m + k_2 t^{2m} \tag{18}$$

where M_t/M_∞ represents the drug fraction released in time t (< 60%), *k1* and *k2* the kinetic constants associated with diffusional and relaxational release, respectively, and m is the purely Fickian diffusion exponent. For the geometry of our devices m = 0.475 was appropriate. To calculate the percentage of drug release due to the Fickian mechanism, the following equation was introduced:

$$F = \frac{1}{1 + (k_2/k_1) \cdot t^m} \tag{19}$$

F is the Fickian release fraction released due to the Fickian mechanism. The ratio of relaxation to the Fickian contributions (R/F) can be expressed as follows:

$$\frac{R}{F} = \frac{k_2}{k_1} \cdot t^m \tag{20}$$

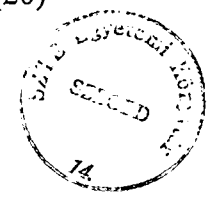

- ***Release profiles comparison***

In order to compare the dissolution profiles of the samples, two fit factors were determined, as described by Moore and Flanner [102]. The difference factor (f_1) measures the percent error between two curves over all time points:

$$f_1 = \frac{\sum_{j=1}^{n} |R_j - T_j|}{\sum_{j=1}^{n} R_j} \times 100 \qquad (21)$$

where n is the sampling number, R_j and T_j are the percent dissolved of the reference and test products at each time point j.

The similarity factor (f_2) as defined by FDA and EMEA is a logarithmic reciprocal square root transformation of one plus the mean squared differences of drug percent dissolved between the test and the reference products [96, 102]:

$$f_2 = 50 \times \log\left\{\left[1 + (1/n)\sum_{j=1}^{n} |R_j - T_j|^2\right]^{-0.5} \times 100\right\} \qquad (22)$$

In general, f_1 values lower than 15 (0-15) and f_2 values higher than 50 (50-100) show the similarity of the dissolution profiles.

5. RESULTS

5.1. Characterization of starch samples subjected to microwave irradiation

The objective of the experiments presented in this chapter was to investigate the morphological parameters and the structural changes of **potato (PS)** and **maize (MS) starches** subjected to microwave irradiation. The effects of volumetric heating and following storage on the moisture content, sorption behaviour and swelling properties of the model substances were examined. The influence of the electromagnetic irradiation on the tensile strengths and surface free energies of compacts pressed from the modified PS and MS was also studied. The initial samples and samples treated by conventional heating were used to

compare the effects of microwave irradiation on the examined properties and parameters of these starches.

The particles of the initial PS (23-75 μm) were ovoid and had a smooth surface (Fig. 12a). The microscopic pictures of PS subjected to microwave irradiation did not reveal noteworthy changes (Fig. 12b). Heating of potato starch at 130 °C caused cracks in the surface of the particles (Fig. 12c).

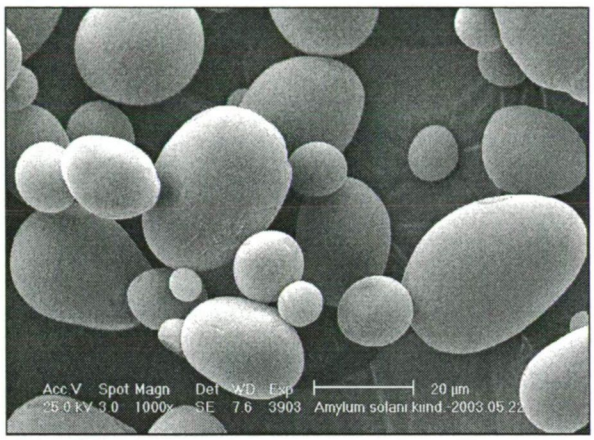

12a. PS

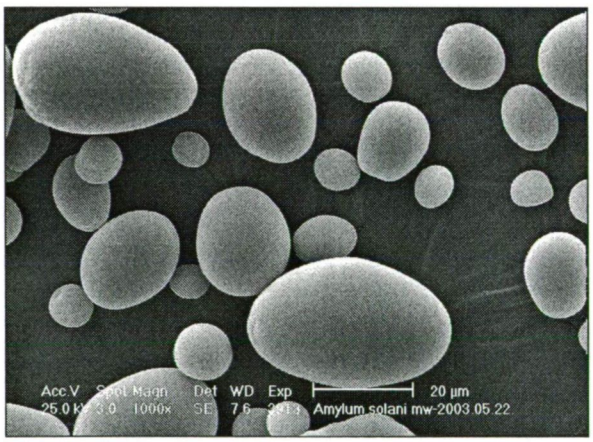

12b. PS_{mw}

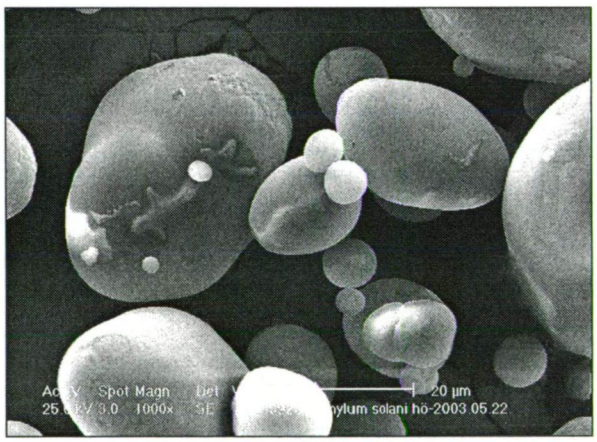

12c. $PS_{130°}$

Figure 12 SEM pictures of potato starch.

The particles of the MS were smaller (9-23 μm) and had a crystalline appearance (Fig. 13a). The initial MS sample consisted of non-agglomerated crystalline particles. The particles were deformed after microwave irradiation (Fig. 13b) and conventional heating, and formed loose agglomerates (Fig. 13c) [**II**]. These observations are in good agreement with the results obtained by Palasinski et al. [103].

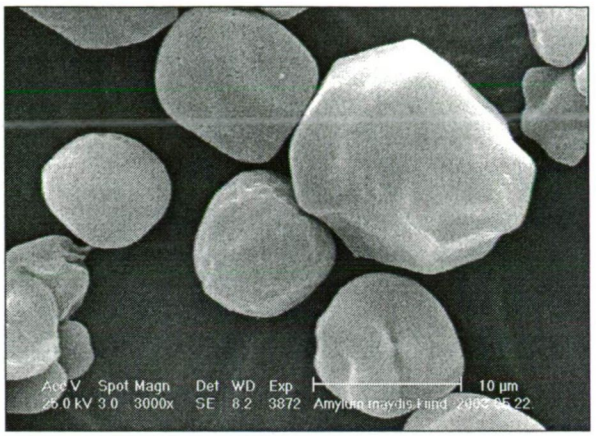

13a. MS

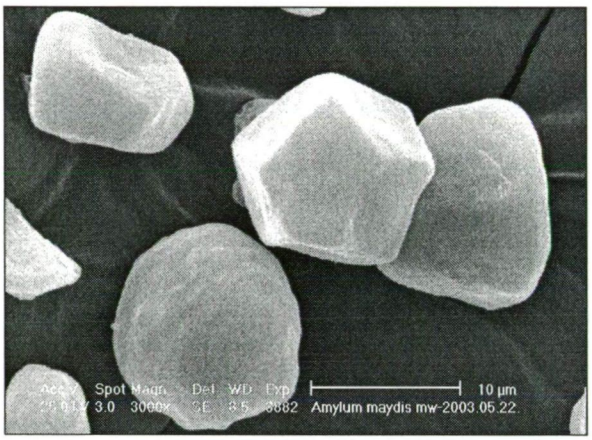

13b. MS_{mw}

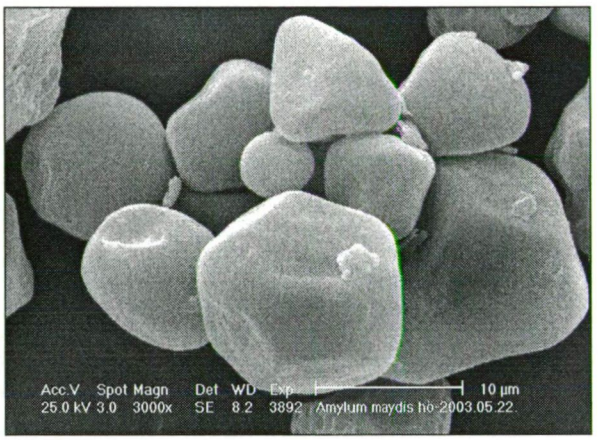

13c. $MS_{130°}$

Figure 13 SEM pictures of maize starch.

The physical treatments applied did not cause remarkable changes in particle size and particle size distribution of the polymers (Table 3). The micromorphological parameters of PS and MS were entirely different (Table 3), which can be related to the structural differences of the samples (see Chapter 3.1.) [3].

The micromeritics of PS were changed slightly during the thermal processes. The specific surface area of the MS processed by conventional heating ($MS_{130\,°C}$) became 40% larger and a similar significant increase was observed on evaluation of the mesopore volume data (30%). The changes in micromorphology of MS were considerable smaller after microwave irradiation (MS_{mw}). Differences between the microstructures of the starch samples are well demonstrated by the cumulative mesopore volume distribution curves (Fig. 14).

Table 3 Parameters of starch samples (n=3).

Samples	$D_{10\%}$ [μm]	$D_{90\%}$ [μm]	S_{BET} [m^2/g]	$V_{P\ 1.7\text{-}300\ nm}$ [m^3/g]*10^{-4}	D (4V/F) [nm]
PS	23.47±0.08	75.62±0.07	0.12±0.002	1.83	11.5
PS_{mw}	23.16±0.02	73.86±0.07	0.10±0.003	1.66	7.55
$PS_{130\ °C}$	23.82±0.30	73.16±0.04	0.11±0.002	1.73	8.47
MS	9.39±0.22	23.02±0.31	0.27±0.004	9.11	13.50
MS_{mw}	9.33±0.01	22.51±0.07	0.30±0.003	9.17	13.00
$MS_{130\ °C}$	9.34±0.02	22.41±0.14	0.38±0.003	11.60	9.42

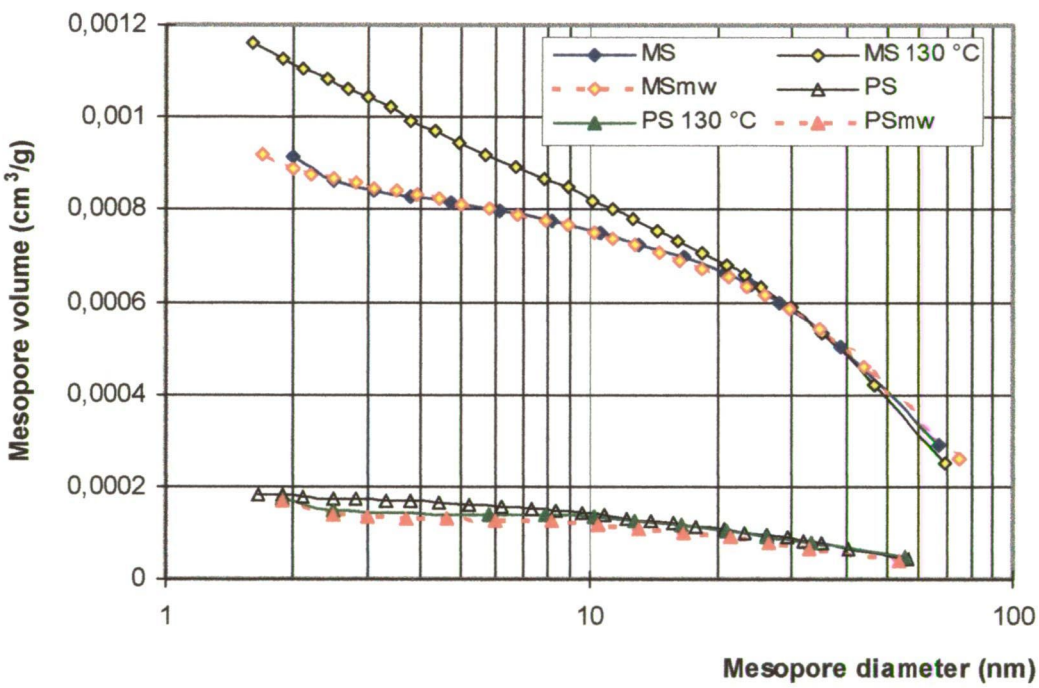

Figure 14 Cumulative mesopore volume distributions of starch samples as a function of average mesopore diameter.

Both microwave irradiation and conventional heating destroyed the crystalline structure of PS (Fig. 15), while MS retained its original X-ray pattern after thermal treatments (Fig. 16).

The results of X-ray diffraction obtained on MS are in accordance with those of previous studies, which reported that the effect of microwave irradiation is less pronounced on cereal

starches containing a lower amount of water molecules in the unit cell and exhibiting an A-type XRPD diffractogram [103-106].

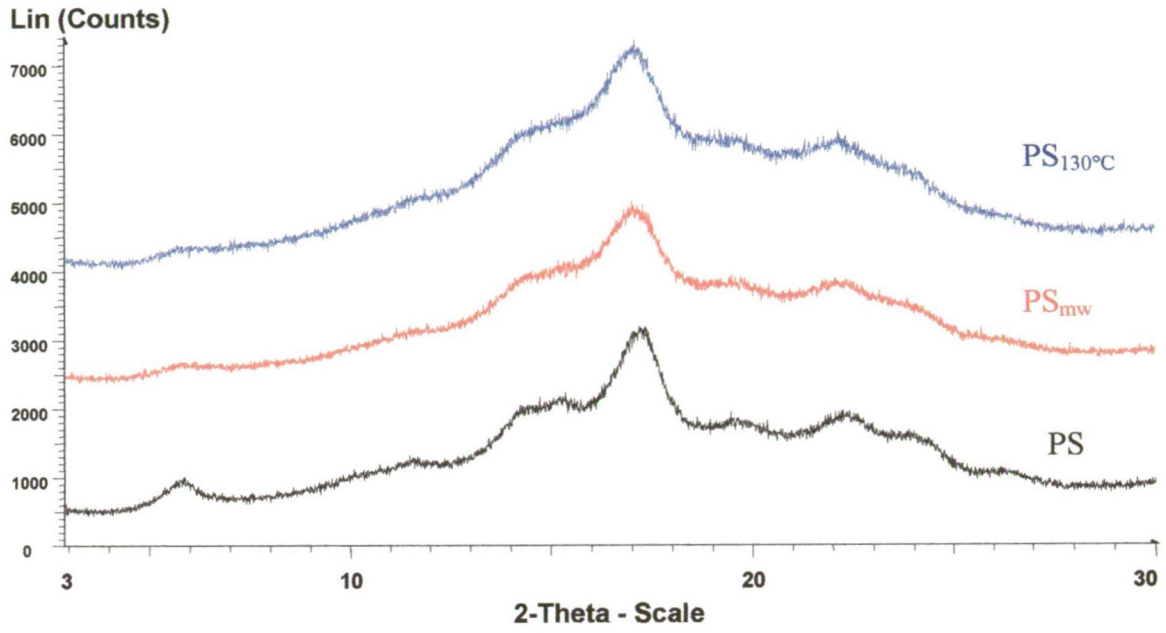

Figure 15 X-ray patterns of potato starch subjected to hydrothermal treatments.

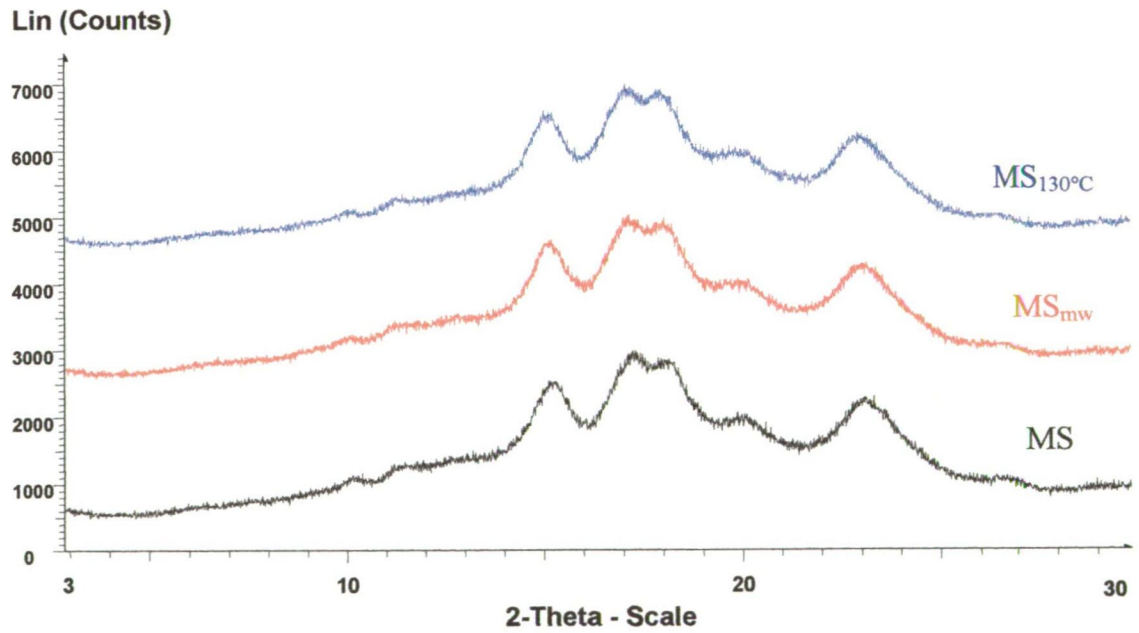

Figure 16 X-ray spectra of maize starch subjected to hydrothermal treatments.

Both microwave irradiation and conventional heating resulted in a significant decrease in the moisture content of PS and of MS. The two types of thermal treatment led to significantly different moisture contents (Table 4) [**III**].

Table 4 Moisture contents of starch samples after thermal treatments and during storage (n=3).

Sample	Moisture content [mg/g starch]				
	Native sample	After thermal treatment	Day 1 of storage	Day 2 of storage	Day 3 of storage
PS	**73.60±2.11**	-	-	-	-
PS_{mw}	-	0.70±0.00	7.30±0.71	27.90±1.51	36.60±0.10
$PS_{130°C}$	-	5.97±1.10	11.57±0.95	28.07±1.93	37.87±0.83
MS	**66.67±2.35**	-	-	-	-
MS_{mw}	-	0.00±0.00	15.40±1.31	36.15±0.78	41.27±2.74
$MS_{130°C}$	-	7.09±0.74	17.47±1.91	32.73±0.96	45.10±2.18

The moisture contents after thermal processing were in accordance with the findings of previous studies that volumetric heating (microwave) allows sufficient energy transfer and hence rapid and uniform heating [9, 11]. The moisture loss resulting from these thermal treatments proved to be reversible, as expected [107]. The processed samples readsorbed a considerable proportion of their initial moisture content during storage. The values of moisture content measured on the first three days of storage are included in Table 4. The rate, at which the samples adsorbed moisture, was determined by weighing the samples at given intervals. The moisture uptake rate (MUR) was determined as the slope of the linear segment [108] (Table 5).

Table 5 MUR values of starch samples (n=3).

Sample	Equation	R^2	MUR [mg/g/day]
PS_{mw}	y = 12.83 x – 1.12	0.9596	12.83
$PS_{130°C}$	y = 11.219 x + 4.039	0.9693	11.22
MS_{mw}	y = 18.075 x – 0.8917	0.9928	18.07
$MS_{130°C}$	y = 13.93 x + 6.203	0.9952	13.93

Our measurements indicated that the first few days after thermal processing play an important role in the moisture uptake of the samples. PS had readsorbed 50% of its initial moisture content by the third day of storage, while MS had readsorbed 70%. It was noteworthy that the MUR of MS was always higher than that of PS.

In the structure of starches, amorphous regions alternate with crystalline micelles, forming a sponge-like structure. Apart from polysaccharides, an integral part of starches is water. According to Bogracheva et al., the degree of crystallinity is linearly proportional to the water content of the polymers and the driving force for increased water uptake is the formation of crystallites [107]. Since the water molecules are adsorbed by the amorphous parts of starches, the moisture content plays an important role in the crystalline - amorphous transformation of these biopolymers [1, 109]. Hence, it is clear that hydrothermal treatment is accompanied by the structural destruction and amorphous transition of PS, due to the dehydration of the sample [110].

Amorphous regions in crystals are generally thermodynamically unstable, i.e. they are in a higher energy state than that for the crystalline form. Within these amorphous regions, the substantial absorption of water vapour can occur, which can cause physical and chemical transitions. The amorphous regions are hot spots in which physical changes and/or chemical degradation can be initiated [111, 112]. Consequently, besides the hygroscopicity of starches, the structural conversion of PS can also contribute to the fast moisture uptake during storage. Since the structure of MS was not considerably influenced by the hydrothermal treatments, the faster water uptake and the higher MUR of MS can be attributed to the micromorphological parameters of the sample: the specific surface area of MS is 3 times higher than that of PS [**II**].

Appreciable differences were observed between the WRC, SC and SP values of the initial samples (PS and MS), which can be explained with the structural differences between these starches of different botanical origins (A- and B-type starches) (Table 6) [79, 80, 88].

The thermal treatments increased the WRC, SC and SP values of PS significantly. The WRC and the SP of PS processed and stored for 6 months ($WRC_{after\ storage}$) was makedly higher than that of the initial sample. Hence, the effect of microwave irradiation on the above-mentioned parameters of PS may be irreversible. In contrast with the WRC and SP values, the increase in SC proved reversible during storage. The results included in Table 6 show that the applied hydrothermal processes did not have a significant influence on the WRC and swelling properties of MS. However, a significant decrease in WRC of MS could be detected after storage of the processed samples.

The increases in the WRC and the swelling parameters of PS may also be related to the crystalline - amorphous transition of the polymer structure and to the reduction in the amylose content ("amylose-escape") initiated by the thermal treatment [7, 92, 103-105]. Moreover, the damage on the surface of starch particles subjected to conventional heating ($PS_{130°C}$) can facilitate the interaction of amylopectin and water molecules during swelling and hence contribute to the increase in SC [**II**]. The reversible change in SC, characterizing the ability of starches to swell in cold water, permits the conclusion that there is a correlation between the decrease of SC and the water uptake during storage.

Table 6 Swelling parameters of starch samples (n=3).

Sample	WRC_{after} thermal treatment	WRC_{after} storage	SC_{after} thermal treatment	SC_{after} storage	SP_{after} thermal treatment [g/g]	SP_{after} storage [g/g]
PS	**1.19±0.01**	-	**1.05±0.04**	-	**28.20±1.29**	-
PS_{mw}	1.73±0.03	1.80±0.21	1.30±0.06	1.10±0.06	37.73±1.80	32.15±1.21
$PS_{130°C}$	1.72±0.06	1.52±0.10	1.53±0.05	1.24±0.08	35.60±0.71	30.87±1.73
MS	**1.63±0.14**	-	**0.77±0.06**	-	**13.83±1.53**	-
MS_{mw}	1.53±0.03	1.35±0.24	0.83±0.00	0.79±0.00	15.41±1.83	13.45±1.57
$MS_{130°C}$	1.85±0.05	1.31±0.12	0.84±0.05	0.75±0.00	13.22±0.49	13.02±1.52

As compared with the compacts consisting of microcrystalline cellulose only (AV), the application of the initial starches for tablet formulation decreased the tensile strengths of the compacts, and the tensile strengths were also decreased after physical treatments (Table 7). The extent of the decrease did not depend on the type of starch applied, but the effects of the thermal treatments on the tensile parameters differed. The decrease in the tensile strength caused by the application of thermally modified PS was more significant than the decreases in the strength parameters of the comprimates containing physically treated MS. The experimental results of MS could be related to its special structure. MS is more resistant towards modifying agents than is PS, which is probably due to the occurrence of lipids in the surface and helical amylose complexes [79, 113].

Table 7 Influence of starches on physical parameters of compacts containing 20% starch and 80% microcrystalline cellulose (Avicel® PH 101) (compression force = 2±0.5 kN) (n=10).

Compacts	Average mass [g]	Average height [mm]	Average tensile strength [MPa]
Avicel® PH 101 (AV)	0.2157±0.0050	2.33±0.02	5.46±0.09
AV/PS	0.2149±0.0012	2.51±0.02	4.60±0.24
AV/PS$_{mw}$	0.2237±0.0012	2.64±0.01	4.00±0.22
AV/PS$_{130\,°C}$	0. 2172±0.0011	2.79±0.01	3.46±0.13
AV/MS	0.2099±0.0031	2.34±0.04	4.83±0.44
AV/MS$_{mw}$	0.2158±0.0073	2.40±0.05	4.31±0.35
AV/MS$_{130\,°C}$	0.2224±0.0011	2.48±0.02	4.43±0.14

The solids containing the initial PS had smaller contact angles than those compressed from the native MS (Table 8). The lower hydrophilicity of MS could be attributed to the lipid content and the special structure of this starch type [114].

Table 8 Contact angles and surface free energies of compacts with a porosity of 10±2% containing 20% starch and 80% microcrystalline cellulose (Avicel® PH 101) (compression force = 20±1 kN) (n=10).

Compacts	Θ_{water} [°]	$\Theta_{diiodo\text{-}methane}$ [°]	γ^d [mN/m]	γ^p [mN/m]	γ [mN/m]	Polarity* [%]
Avicel® PH 101 (AV)	38.83±1.77	25.02±0.66	33.69	27.81	61.49	45.23
AV/PS	33.00±1.40	24.46±0.70	32.72	31.72	64.44	49.22
AV/PS$_{mw}$	47.20±1.97	33.08±0.77	31.81	23.28	55.09	42.26
AV/PS$_{130\,°C}$	44.84±1.02	37.59±1.65	31.87	25.21	57.08	44.17
AV/MS	34.47±1.78	25.24±1.12	33.21	30.60	63.80	47.96
AV/MS$_{mw}$	45.03±1.48	33.13±1.20	31.44	25.33	56.77	44.62
AV/MS$_{130\,°C}$	53.51±1.76	32.05±1.53	30.90	20.19	51.09	39.52

*Polarity = (γ^p/γ) *100 [115]

The effects of the microwaved PS and MS on the contact angles were significant and had the same scale, while application of the MS treated by conductive heating resulted in larger changes in the contact angles than those for the PS. The decreased hydrophilicity of the processed starches could be explained by the fact that thermal treatment decreases the content of the more hydrophilic structure polymer ('amylose-escape') [103-105].

Both the microwave irradiation and the conventional heating reduced the surface free energy and the polarity of the compacts, which was due to the water loss from the starches caused by the thermal treatment. The disperse and polar parts of the surface free energies of the initial samples were nearly equal. After the thermal processes, the polar components fell drastically, whereas the disperse part did not decrease significantly (Table 8).

Conclusion

Volumetric heating resulted in reversible moisture loss from both types of samples. The crystallinity of potato starch was decreased, while its water retention capacity and swelling power were increased irreversibly, and its swelling capacity was increased reversibly by the thermal process applied. The corresponding parameters of maize starch were not influenced significantly by volumetric heating; this may be related to its special structure resulting in the thermal resistance of this polymer.

The results presented in this work allow the conclusion that the difference in response of PS and MS to the microwave irradiation was related to the structural difference of the initial starches. The changes in tensile strength, wettability and surface free energy could be attributed to the water loss (dehydration) during microwave treatment. On the other hand, irreversible structural changes caused by the physical treatments, such as crystalline-amorphous solid phase transition and "amylose escape" may have an influence on the above properties. Although microwave irradiation is known not to influence molecular structure, these results allow the conclusion that a profound knowledge of the effects of microwave irradiation on the physico-chemical properties of frequently used excipients is essential in order to rationalize the use of dielectric heating for pharmaceutical processing.

As concerns the practice of drug formulation, it can be concluded that, apart from the optimum drying parameters, adequately controlled storage conditions are also of vital importance in ensuring the appropriate moisture content of starches and pharmaceutical formulations containing starch.

For the microwave drying of pharmaceutical formulations, the application of maize starch is advisable, with regard to the thermal resistance of this polymer. Microwave irradiation can be regarded as a suitable and selective non-conventional method for the purposeful physico-chemical modification of potato starch.

5.2. Formulation and characterization of a solid dosage form prepared via the freeze-casting technique

The aim of the present work was to develop a fast-dissolving solid dosage form containing theophylline as active ingredient and potato starch as filler using the freeze-casting technique. The structure, the physical properties and mechanism of drug release from the freeze-casted units were investigated. The examined properties of the samples were compared with those of tablets compressed by an eccentric tableting machine using three different compression forces.

Physical properties of the aqueous suspensions, such as viscosity, play an important role in the freeze casting process. The first step of the sample preparation was the production of an appropriate aqueous suspension, which exhibited a good flowability (it could be poured into the moulding form without difficulty), whereas the sedimentation of the suspended particles during the freezing process was negligible **[V, VI]**. The suspensions can be characterized by thixotropic flow (Fig. 16). Thixotropic systems exhibit easy flow at relatively high shear rates. However, when the shear stress is removed the system is slowly reformed into a structured vehicle. The usual property of thixotropy results from the breakdown and build up of floccules under stress. The primary advantage of thixotropic flow is that it confers pourability under shear stress and viscosity when the shear stress is removed at rest [116]. The viscosity of each system at a shear rate of 100 s^{-1} is included in Table 1 (see Chapter 4.1.).

It is well known that starches swell and form gels in excess water during heating. Therefore, the pasting temperatures of the suspensions were determined and the drying temperatures of the samples were kept under the gelatinization temperatures. The gelatinization temperatures of the samples are given in Table 1 (see Chapter 4.1.).

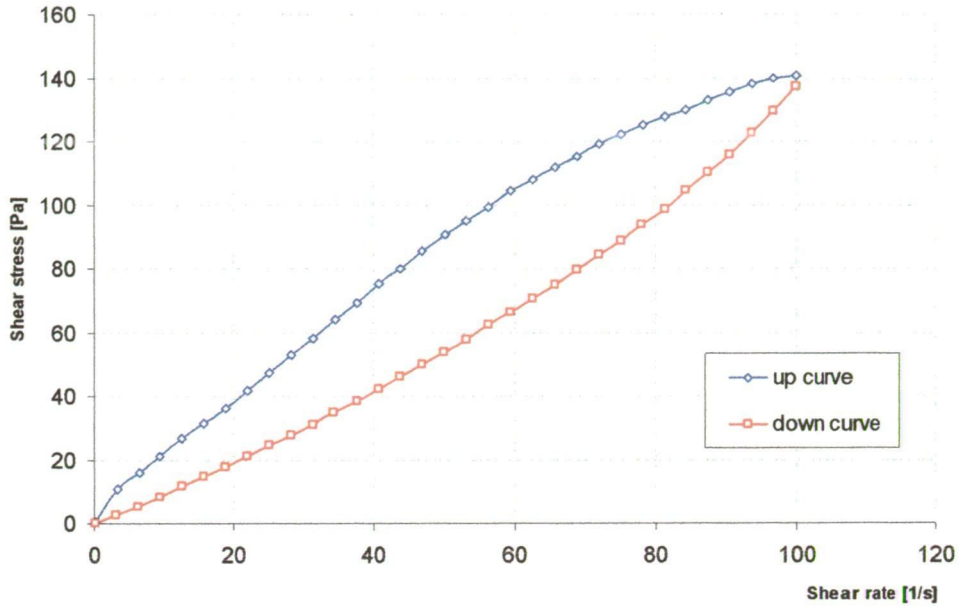

Figure 16 Flow curve of an aqueous suspension containing potato starch and theophylline (Sample 1).

A solid dosage form produced by freeze-casting is depicted in Figure 17. Sample 1 was very fragile and difficult to handle. The data given in Table 9 justify that the tensile strength of the freeze-casted samples is notably lower than that of the tablets compressed with an eccentric tableting machine. The tensile strength values of the tablets show a very good correlation with the applied compression force.

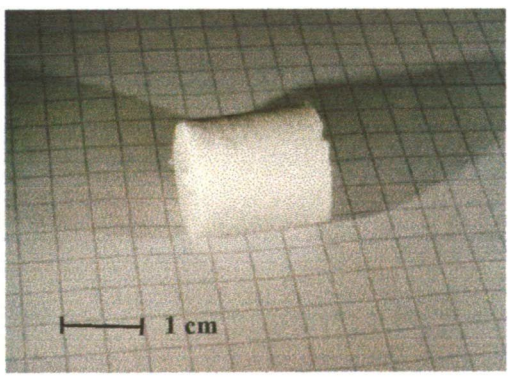

Figure 17 Picture of a starch matrix without an active ingredient produced by freeze-casting.

Table 9 Physical parameters of Sample 2 (n=10), Sample 3 (n=10) and the tablets (n=20).

Samples	Average weight [g]	Average diameter [mm]	Average height [mm]	Average tensile strength [MPa]	Moisture content [% (w/w)]
Sample 2	1.447 ± 0.209	14.32 ± 0.21	10.34 ± 1.61	0.29 ± 0.06	6.95 ± 0.27
Sample 3	1.456 ± 0.252	14.51 ± 0.93	10.04 ± 2.63	0.32 ± 0.05	7.31 ± 0.29
Tablet/5 kN	0.248 ± 0.010	10.02 ± 0.01	2.81 ± 0.04	1.94 ± 0.34	_
Tablet/10 kN	0.250 ± 0.026	10.01 ± 0.01	2.63 ± 0.07	2.92 ± 0.45	_
Tablet/20 kN	0.255 ± 0.010	10.01 ± 0.01	2.60 ± 0.07	4.03 ± 0.33	_

Figure 18 shows the fine porous structure of the freeze-casted matrices. Figure 19 demonstrates the surface characteristics of the samples containing theophylline and the additives. The SEM micrographs exhibit the needle-like crystals of the active pharmaceutical ingredient and the ovoid particles of potato starch.

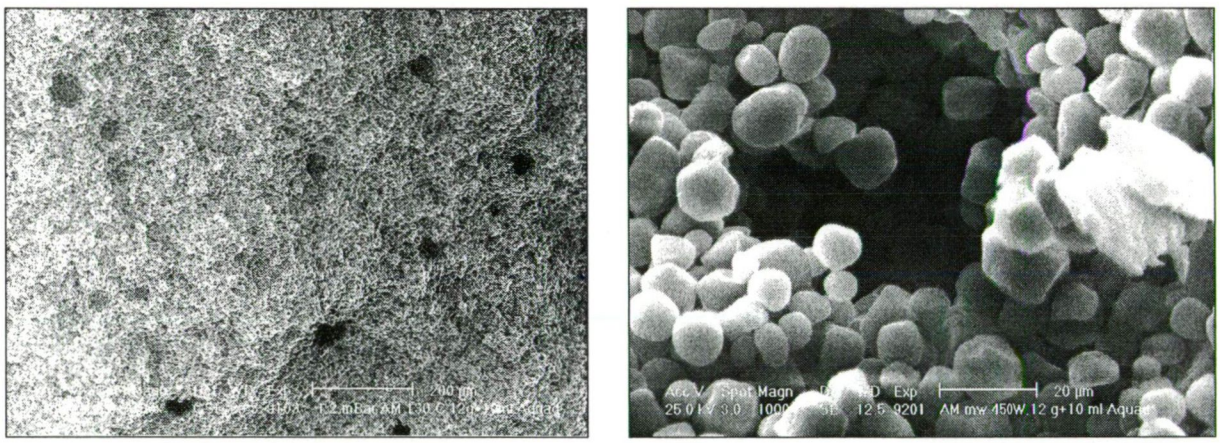

Figure 18 SEM pictures of starch-based matrices without an active ingredient.

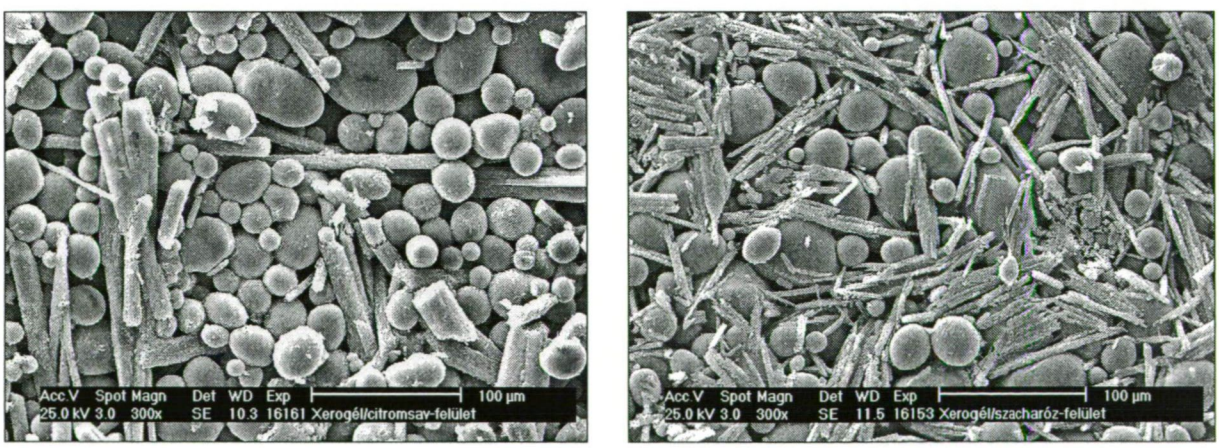

19a. **19b.**

Figure 19 SEM pictures of the surface of Sample 2 (19a) and Sample 3 (19b).

The SEM pictures reveal that starch particles remained intact during drying and the freeze-casted matrix is stabilized by contact points formed by the water-soluble additives (saccharose and citric acid) recrystallized during the evaporation of water (binding-effect of the additives) (Fig. 20) [117].

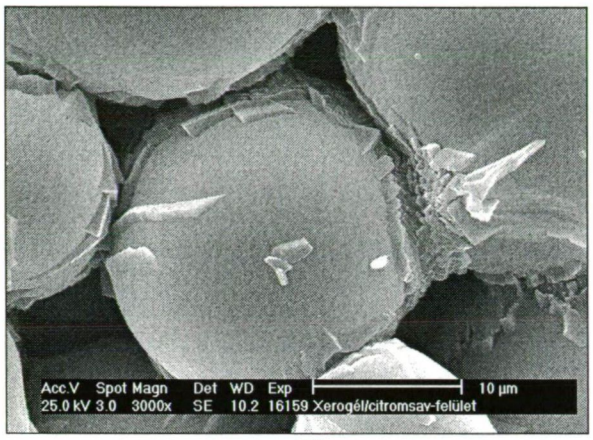

20a.

20b.

Figure 20 SEM pictures of Sample 2 (20a) and Sample 3 (20b) produced by freeze-casting.

The results of the porosity measurements confirmed the porous nature of the freeze-casted samples compared to tablets compressed with different compression forces (Table 10). The total volume of mercury (V_{tot}) intruded into the freeze-casted units was markedly higher than that intruded into the tablets. Significant differences could also be observed between the porosity percentages (ε) and the pore sizes (d_{mean}) of the matrices and the tablets.

Table 10 Micromorphological parameters of the freeze-casted samples and the tablets compressed with different compression pressures (n=3).

Sample	Total intruded volume (V_{tot})	Total pore surface area (S)	Mean pore diameter (d_{mean})	Specific surface area (S_{BET})	Apparent particle density (ρ_h)	Porosity (ε)
	[cm^3/g]	[m^2/g]	[nm]	[m^2/g]	[g/cm^3]	[%]
Sample 2	0.45 ± 0.02	1.07 ± 0.02	1676 ± 65	0.15 ± 0.01	1.92 ± 0.01	46.27
Sample 3	0.29 ± 0.02	1.19 ± 0.03	975 ± 80	0.20 ± 0.01	1.92 ± 0.01	35.81
Tablet/5 kN	0.18 ± 0.01	1.26 ± 0.02	569 ± 22	0.86 ± 0.01	1.91 ± 0.01	22.82
Tablet/10 kN	0.11 ± 0.01	1.37 ± 0.03	332 ± 19	0.80 ± 0.01	1.91 ± 0.01	17.92
Tablet/20 kN	0.09 ± 0.01	1.33 ± 0.02	267 ± 10	0.79 ± 0.01	1.91 ± 0.01	14.49

Figure 21 shows the cumulative pore volume distribution, while Figure 22 demonstrates the pore volume size frequency obtained by combination of the results determined with nitrogen adsorption and mercury porosimetry [**IV**].

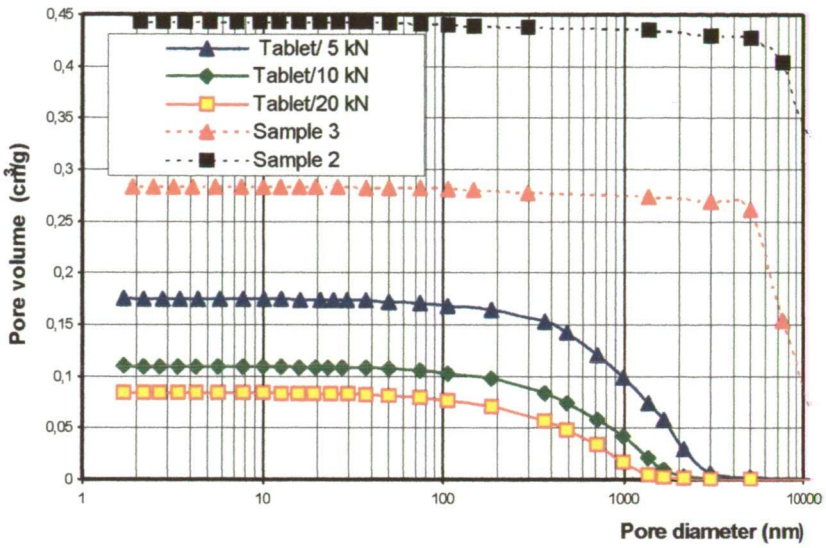

Figure 21 Cumulative pore volume - size distribution curves obtained by combination of the results determined with nitrogen adsorption and mercury porosimetry.

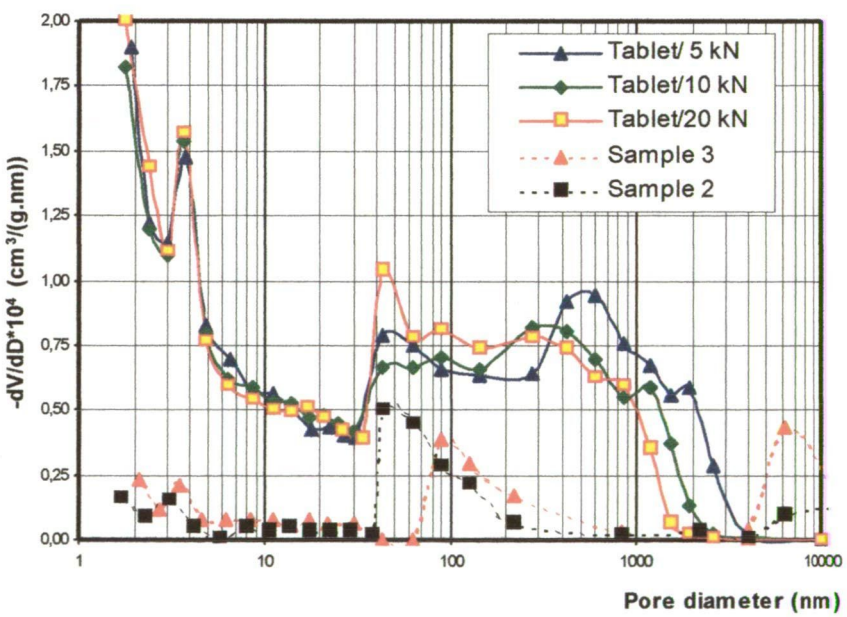

Figure 22 Pore volume (V) – size (D) frequency curves obtained by combination of the results determined with nitrogen adsorption and mercury porosimetry.

Considering the pore size, tablets contained some meso- and macropores, while the dendritic structure of the freeze-casted samples included only macropores (Fig. 21). The total pore

volume of Sample 2 and Sample 3 can be originated from the pores having a diameter larger than 1 μm. The larger mean pore diameter of the matrices (d_{mean}) corresponds to higher porosity (ε) and smaller total pore surface area (S; S_{BET}) (Table 10).

Pore volume size distribution curves (Fig. 22) emphasize differences of the pore volume at small pore size intervals. High frequency of mean pore diameters of tablets in the 2-5 nm range could imply some pores with this entrance diameter range and a wide inner body (ink-bottle pores), rather than a large number of pores with these dimensions.

The surface area values obtained by mercury porosimetry (S) are significantly higher than those obtained by nitrogen adsorption (S_{BET}) (Table 10). This is due to the complex pore structure and the ink-bottle-shaped pores of the tablets. The surface area in mercury porosimetry is calculated from the volume intruded in pore diameter intervals assuming cylindrical pores with round pore openings. The so-called ink-bottle pores tend to increase surface area values calculated from mercury porosimetry data, because the volume of the pores with small necks can be remarkable [83-85, **IV**].

Furthermore, it should be pointed out that a significant difference was found between the micromeritics of Sample 2 and Sample 3. Hence, effects of the binding materials on the microstructure may be assumed.

The results of the dissolution study revealed the rapid delivery of theophylline from the matrices as compared with the rate of dissolution from the tablets (Fig. 23).

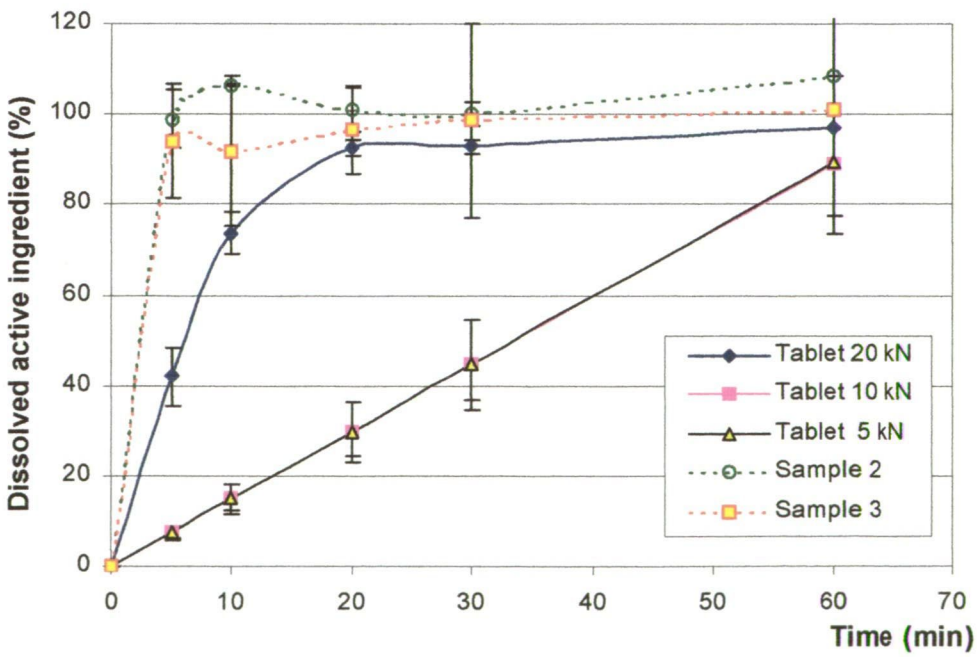

Figure 23 Profile of theophylline dissolution in artificial gastric juice.

Figure 23 shows that almost the total amount of the incorporated active ingredient was dissolved from the freeze-casted samples in the first 7 min of the study (burst effect). During this period, only 60% of the theophylline was delivered from Tablet/20 kN and 10% of the active agent was dissolved from Tablet/10 kN and Tablet/5 kN.

The values of the characterized dissolution time (τ) also evidenced the promoted dissolution of Sample 2 and Sample 3 as compared to the tablets (Table 11).

Table 11 Parameters of rates of dissolution by RRSBW distribution.

Sample	β shape parameter	τ value [min]	R^2
Sample 2	6.66	**3.98**	0.9998
Sample 3	2.28	**4.72**	0.9438
Tablet/5 kN	1.13	**48.83**	0.9988
Tablet/10 kN	1.13	**49.15**	0.9988
Tablet/20 kN	0.92	**8.51**	0.9392

The τ value of Tablet/20 kN, which was calculated from the slope and the intercept values after linearized regression and transformation of the Rosin-Rammler-Sperling-Bennett-Weibull distribution, is two times higher than those of the freeze-casted matrices, while the characterized dissolution times of Tablet/5 kN and Tablet/10 kN are more than ten times higher than those of Sample 2 and Sample 3.

The correlation coefficients of different kinetic equations are included in Table 12.

Table 12 Correlation coefficients of different parameters measured and estimated applied the mathematical models.

Sample	Zero-order model	First-order model	Higuchi square-root of time model
Sample 2	0.7634	0.9992	***0.9997***
Sample 3	0.7634	0.9992	***0.9997***
Tablet/5 kN	***1.0000***	0.9973	0.9459
Tablet/10 kN	***1.0000***	0.9973	0.9459
Tablet/20 kN	0.8306	***0.9974***	0.9843

The dissolution mechanisms of Tablet/5kN and Tablet/10kN can be characterized preferably by a zero-order kinetic revealing a constant rate of dissolution, while the release from Tablet/20kN fits mostly to the first-order model. The diffusion-controlled matrix release (Higuchi-model) is most close to Sample 2 and Sample 3.

On the basis of the obtained values of f_1 and f_2 (Table 13), the dissolution profiles of the samples can be considered different compared to the tablets used as references ($f_1 > 15$; $f_2 < 50$), while the profiles of Sample 2 and Sample 3 can be considered the same ($f_1 < 15$; $f_2 > 50$).

Table 13 Fit factor values obtained for the freeze-casted samples and the tablets.

Sample	Difference factor (f_1) [%]	Similarity factor (f_2)
Sample 1 – Tablet/5 kN	122.86	7.59
Sample 1 – Tablet/10 kN	123.19	7.56
Sample 1 – Tablet/20 kN	29.82	26.23
Sample 2 – Tablet/5 kN	118.78	9.55
Sample 2 – Tablet/10 kN	119.13	9.51
Sample 2 – Tablet/20 kN	23.51	30.15
Sample 2 – Sample 3	6.43	56.98

The results of the dissolution study are in accordance with the micromeritics of the samples and indicate that the high porosity resulted by the presence of large macropores allowed a good matrix-solvent interaction and enhanced the dissolution of the active pharmaceutical ingredient from the freeze-casted dosage forms.

The smaller τ values of the tablets may be also explained by their complex pore structure and are in good agreement with previous studies which reported that pores with a narrow neck and a large internal volume (ink-bottle pores) may have a negative influence on drug dissolution rates [118].

The results of the dissolution study indicate a difference between the dissolution kinetics of the tablets (Fig. 23, Table 12). Compared to Tablet/5 kN and Tablet/10 kN the τ value of Tablet/20 kN is considerable lower (Table 11). These differences can be explained by the correlation of compression force and swelling force of starches. According to some authors, the higher the compression force is during the tableting process, the higher the swelling force

of the starch particles is during disintegration. Hence, higher compression force might result in faster disintegration and higher dissolution rates [119-121].

Conclusion

The results of this study permitted the conclusion that the freeze-casting technique is suitable for the formulation of porous dosage forms containing theophylline as an active pharmaceutical ingredient and potato starch as filler.

In accordance with previous studies, the mechanical stability of the samples could be improved by using water-soluble additives, which can stabilize the matrix structure by their recrystallization upon evaporation of the suspending agent. However, the tensile strength values of the freeze-casted units were markedly lower than those of the tablets compressed with an eccentric tableting machine. In order to protect the solid dosage form against mechanical stress, convenient packaging might be an appropriate alternative.

As compared with tablets used as references, the freeze-casted matrices revealed a considerable difference in pore structure and micromeritics.

The results of the dissolution studies demonstrated that the matrix-solvent interaction was enhanced by the large pore size and porous structure of the freeze-casted samples. The initial burst effect was the result of a rapid dissolution and release of theophylline from the matrices into artificial gastric juice.

5.3. Preparation and characterization of starch-based hydrogels prepared by using isostatic ultrahigh pressure

The purpose of this study was to investigate the applicability of ultrahigh pressure for the aim of drug formulation. In this work, aqueous suspensions of potato and maize starches containing theophylline as an active pharmaceutical ingredient were subjected to isostatic ultrahigh pressure (IUHP). The changes in the structure and morphology of potato and maize starches were investigated. The release profile of theophylline from the pressurized samples was also studied.

Preformulation study

Starch-water suspensions pressurized at 300 MPa did not exhibit visible changes. SEM analysis confirmed that the granules of PS and MS treated at 300 MPa retained their granular shape and smooth surface (Figs. 24 and 25).

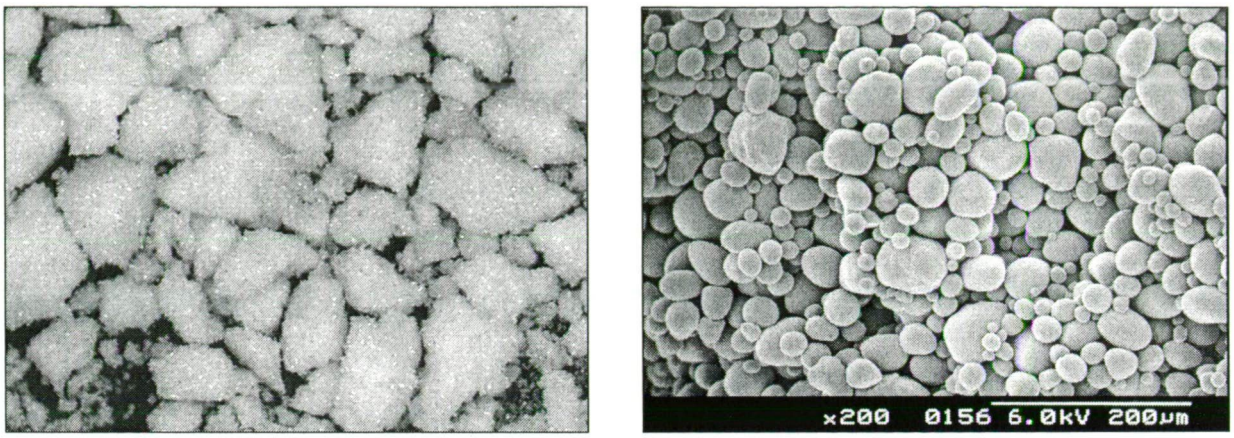

Figure 24 Stereomicrograph (magnification 10x) and SEM picture of $PS_{300\text{-}5}$.

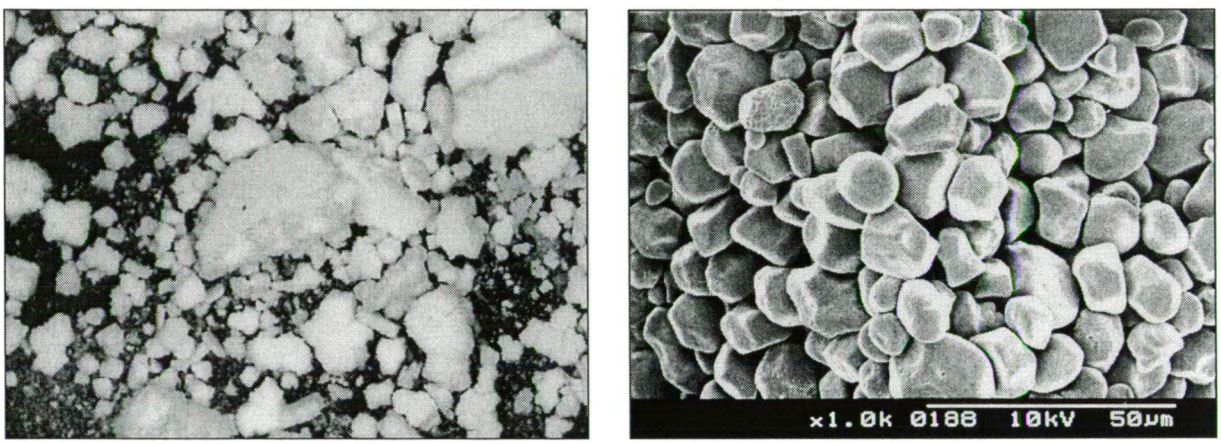

Figure 25 Stereomicrograph (magnification 10x) and SEM picture of $MS_{300\text{-}5}$.

The samples subjected to 700 MPa turned into highly viscous gels, although the temperature in the pressure chamber did not reach the starch gelatinization temperature known from the literature (~72 °C). The majority of the particles of PS pressurized at 700 MPa did not display apparent changes in shape or surface characteristics. However, some particles were characterized by significant surface damage and deformations (Fig. 26).

Treatment at 700 MPa led to an irreversible loss of the particle structure of MS. $MS_{700\text{-}5}$ and $MS_{700\text{-}20}$ revealed a high level of destruction of the particle integrity. Figure 27 demonstrates clear network-like gel structures. These observations are closely related to those of a previous study on high pressure-treated starches [1, 69].

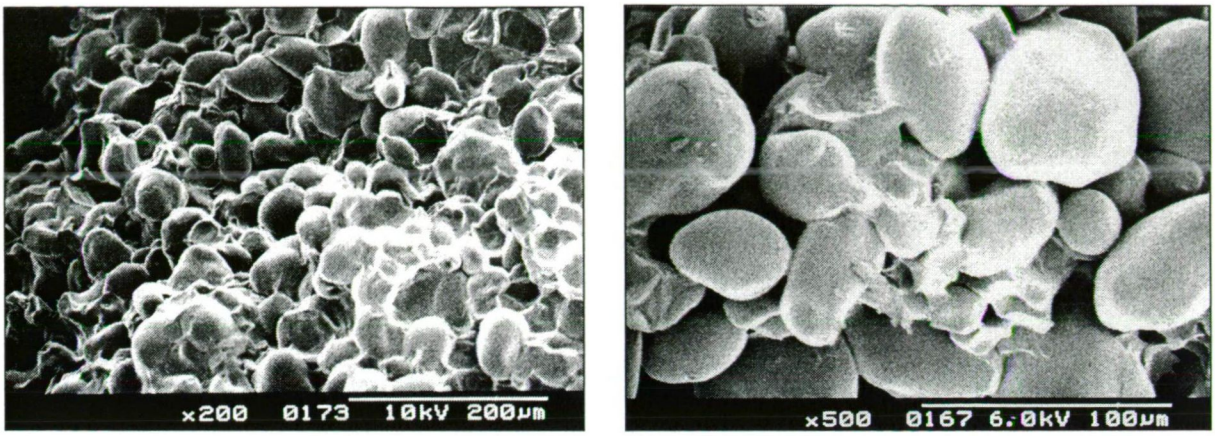

Figure 26 SEM micrographs of $PS_{700\text{-}5}$.

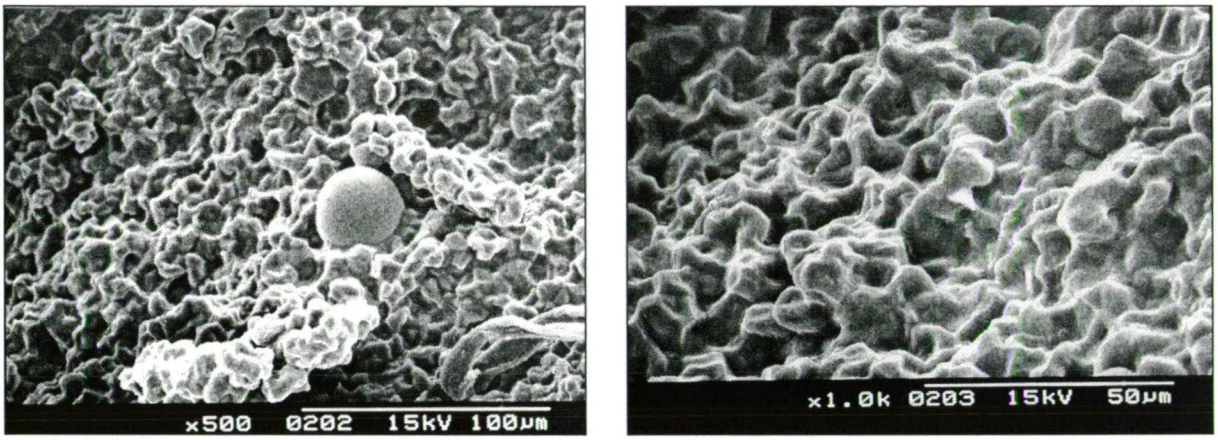

Figure 27 SEM pictures of $MS_{700\text{-}5}$.

As expected from the previous findings, MS (possessing an A-type X-ray powder diffraction pattern) proved to be more sensitive to UHP, while PS (with a B-type crystal structure) was more stable toward IUHP treatment [3, 75, 76]. PS pressurized in aqueous medium retained its original X-ray pattern. Nevertheless, the intensity of the peaks was decreased after treatment at 700 MPa, which can be attributed to the loss of crystallinity during pressurization (Fig. 28).

The X-ray diffractogram of MS pressurized at 300 MPa indicates marked changes (Fig. 29). Figure 29 demonstrates the change in the crystalline structure of MS from A to B type upon treatment at 700 MPa ($MS_{700\text{-}5}$). The single peak at 22° 2θ characteristic of A-type starches remained unchanged. The X-ray curve of $MS_{700\text{-}5}$ reveals a peak at around 6° 2θ and the transformation from a double peak to a single peak at around 17.5°, which are characteristic of the B-type pattern (peaks denoted by arrows) [77, **XIII**].

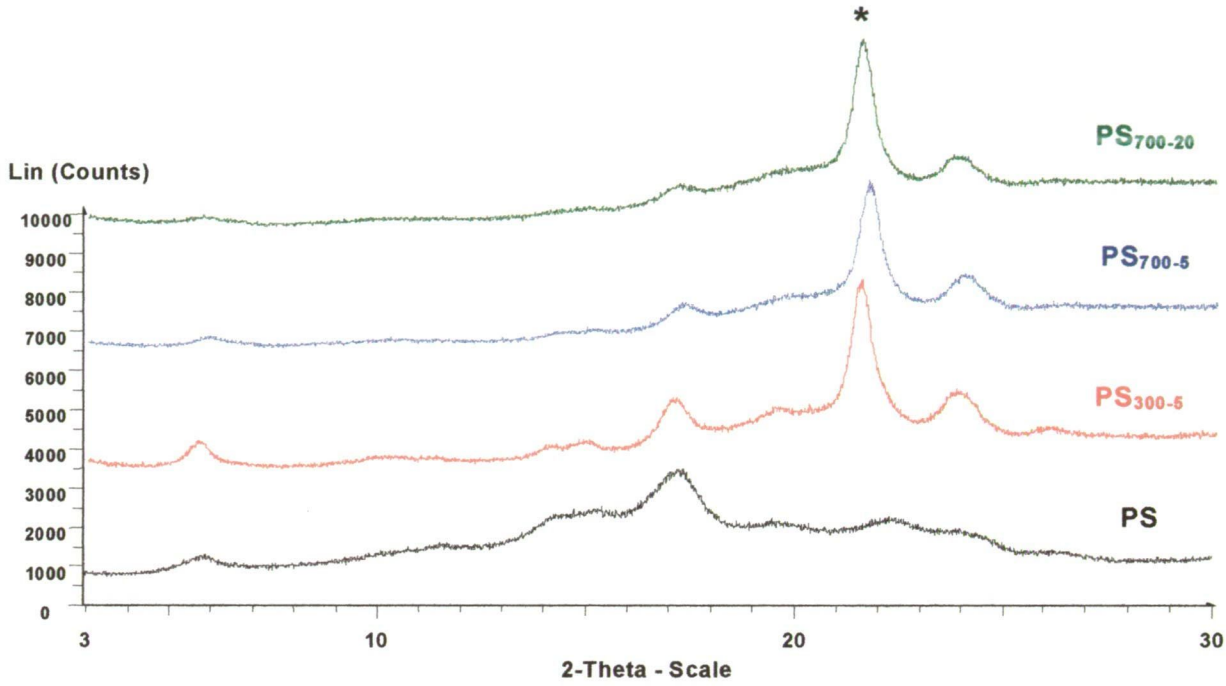

Figure 28 X-ray curves of potato starch samples (*Peak of the sample protection foil).

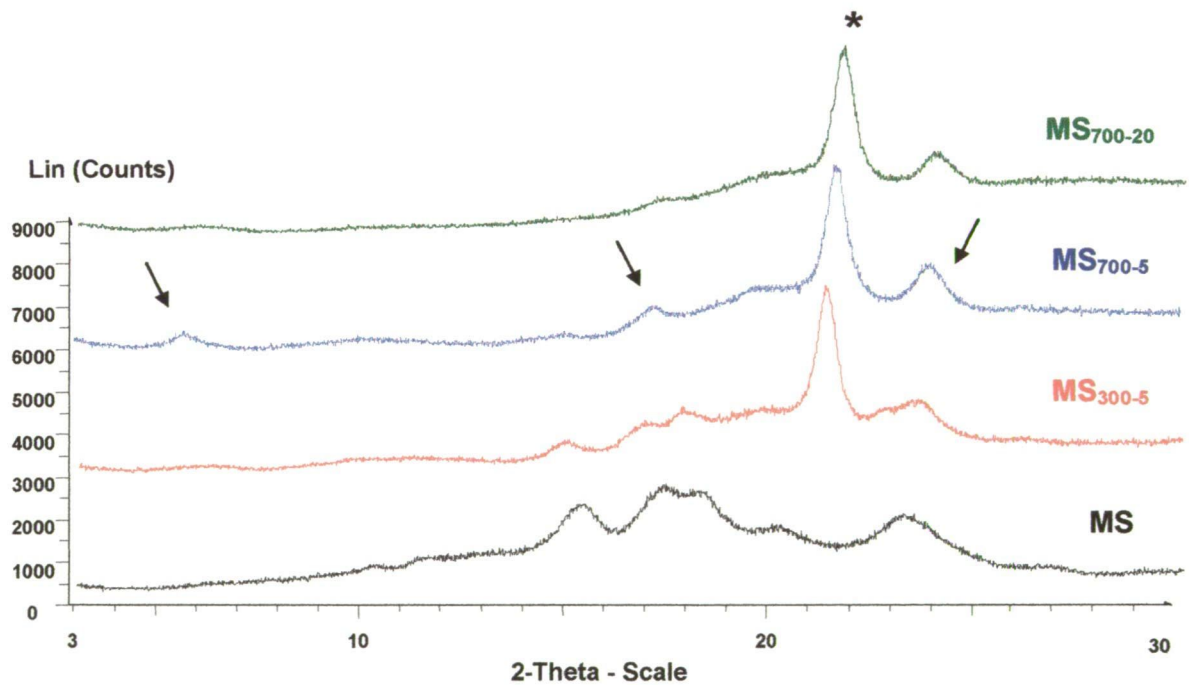

Figure 29 X-ray curves of maize starch samples (*Peak of the sample protection foil).

These observations might be explained in terms of the differences in amylopectin structure and water content of the A-type and B-type starches. In the B-type crystallite, water fills up the channel in the unit cell and stabilizes the crystalline structure. For A-type starches, the

more scattered branching structure of amylopectin is more flexible and allows rearrangements of the double helices, which permits a structure transformation [77].

On the basis of the preformulation studies, pressurization at 700 MPa for 5 minutes was chosen in order to formulate gel samples containing theophylline as an active pharmaceutical ingredient, since the gelatinization of the starch suspensions and the structural conversion of MS occurred completely using the given process parameters.

Investigation of theophylline dissolution from starch gels prepared by IUHP treatment

A considerable difference could be observed between the profiles of theophylline release from the starch gels (**PS-T; MS-T**) and the reference (**T**) (Fig. 30). The correlation coefficients of different kinetic equations are included in Table 14.

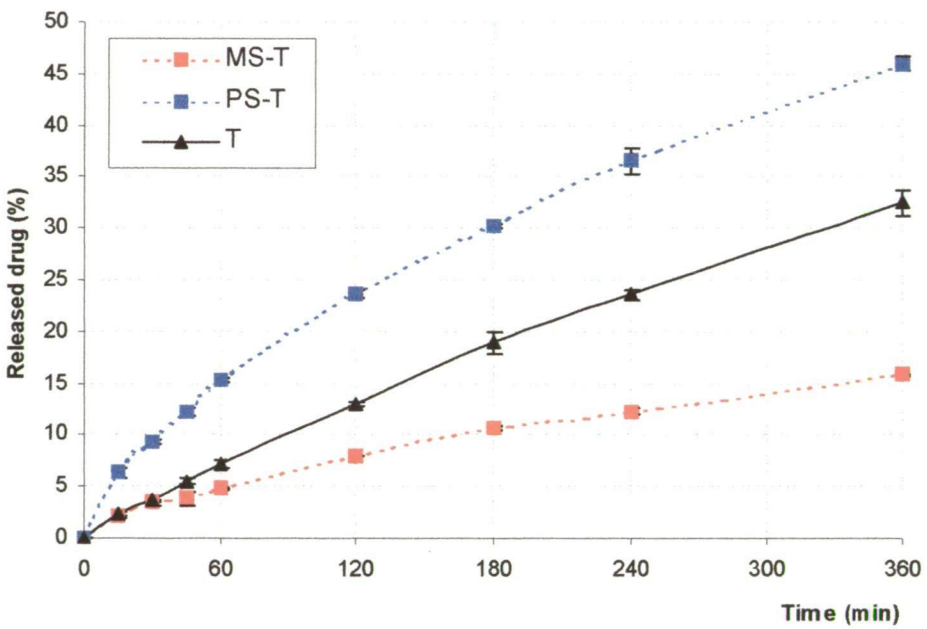

Figure 30 Dissolution profile of theophylline from the gels and the reference (**XVIII**).

The dissolution mechanism from the aqueous theophylline suspension used as a reference (T) can be characterized preferably by a first-order kinetic, while the release from PS-T fits mostly to the Hixson-Crowel model. On the basis of these results, it can be assumed that the drug release from PS-T occurs only in vertical direction relative to the matrix surface and the matrix maintains its original shape during the release progress [96]. The release mechanism of theophylline from MS-T can be characterized with the Korsmeyer-Peppas model.

Table 14 Correlation coefficients of different kinetic equations.

Sample	First order kinetics	Higuchi model	Hixson-Crowel model	Korsmeyer-Peppas model
MS-T	0.9735	0.9468	0.9709	***0.9943***
PS-T	0.9867	0.9321	***0.9922***	0.9606
T	***0.9990***	0.9958	0.9976	0.9989

The results of fitting to Eq. 17 are summarized in Table 15. The diffusional exponent (n = 0.6351) signified a non-Fickian or anomalous mechanism of drug release. Drug dissolution occurring via Fickian diffusion proved to be essential, because the diffusional rate constant (k_1) is much larger than the relaxational constant (k_2) [98-101].

Table 15 Diffusional exponent *(n)* (Eq. 16), diffusional *(k_1)* and relaxational *(k_2)* kinetic constants (Eq. 17) and Pearson's coefficient *(R^2)* for MS-T.

	n	R^2	k_1 [$\%h^{-0.475}$]	k_2 [$\%h^{-0.95}$]	R^2
MS-T	**0.6351**	0.9943	**4.2088**	**0.3754**	0.9987

As shown in Figure 31, the Fickian contribution to the overall release process decreased with increasing amount of released drug. Hence, the relaxation of the polymer chains became more pronounced (Fig. 32).

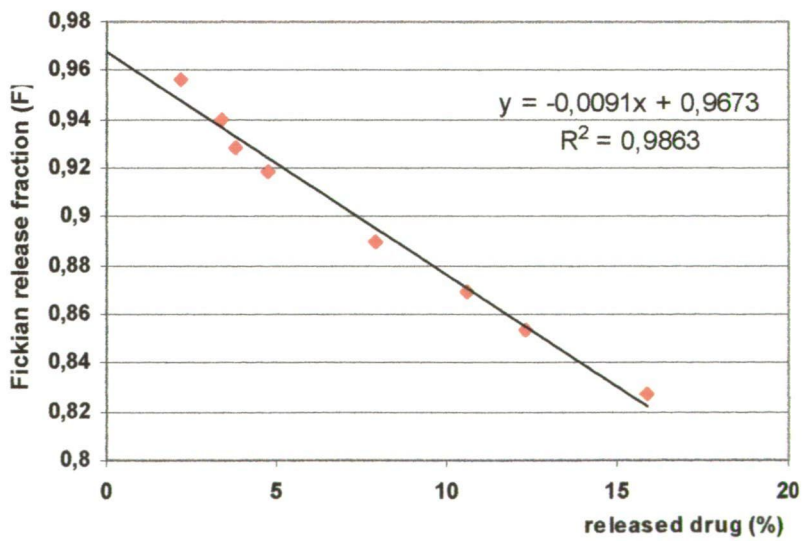

Figure 31 Fickian release fraction (F) (Eq. 19) as a function of released theophylline from MS-T.

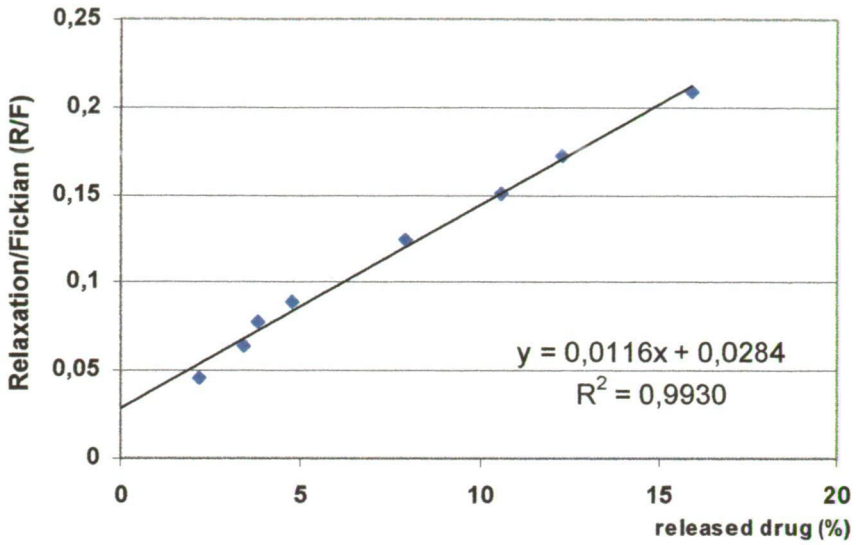

Figure 32 Ratio between relaxational (R) and diffusional (F) contributions to release of theophylline from MS-T (Eq. 20).

These results can be explained with the simultaneous water up-take during the dissolution process, which enables polymer relaxation [99]. It must be noted that the first three measuring points of the dissolution curve of MS-T coincide with those of T, which may be probably due to the presence of free drug particles on the sample's surface easily accessible for the dissolution medium.

The values of the characterized dissolution time (τ) evidenced the promoted drug release from PS-T as compared to the reference (T) (Table 16). The τ value of PS-T is significantly smaller than those of the reference, while the characterized dissolution time of MS-T is more than seven times higher than the τ value of T [97].

Table 16 Parameters of rates of dissolution by RRSBW distribution.

Sample	β shape parameter	τ value [min]	R^2
MS-T	0.6582	**5324**	0.9938
PS-T	0.7171	**734**	0.9982
T	0.9108	**1023**	0.9988

On the basis of the obtained values of f_1 and f_2 (Table 17), the dissolution profiles of the gels can be considered different compared to each other and the reference [102].

Table 17 Fit factor values obtained for the gels prepared by IUHP processing.

Sample	Difference factor (f_1) [%]	Similarity factor (f_2)
MS-T/T	42.86	56.06
PS-T/T	68.25	51.86
MS-T/PS-T	66.04	30.47

According to the literature, the process of drug release in an aqueous medium is strongly influenced by the wettability of the sample's surface [122]. The results of contact angle measurements shown in Table 18 confirmed that the gels containing starches as hydrophilic polysaccharides exhibit smaller contact angle values compared to the pure active drug substance.

Table 18 Contact angle of the samples measured with bidistilled water (Θ_{water}).

Sample	Θ_{water} [°]
MS-T	16.12±0.86
PS-T	16.73±0.81
T	36.13±2.22

Smaller contact angles correspond to better wetting properties, which can contribute to the faster drug release from PS-T. However, the improved wettability of MS-T did not result in promoted drug dissolution. Therefore, it is reasonable to assume that the sustained drug release from MS-T can be attributed to the changes in morphology and structure of the gel-forming polymer caused by IUHP processing.

Conclusion

IUHP treatment of potato and maize starch in presence of water generated highly viscous gels. The process was accompanied by the structural conversion of maize starch. The results of the morphological and structural studies carried out in this work were in good agreement with previous studies, which reported a difference in pressure sensitivity depending on the botanical origin of starch as one of the major benefits of pressure-induced gelatinization.

The profile of drug release from the gels prepared by IUHP processing could be characterized by different kinetics. The hydrogel containing potato starch as a gel-forming polymer exhibited faster drug dissolution compared to the aqueous theophylline suspension used as a reference, while the pressurization of maize starch resulted in a gel exhibiting sustained drug release. Our experimental results allow the conclusion that the morphological and structural changes caused by pressurization have a significant influence on the dissolution process.
The different pressure sensitivities of the starches permit the use of IUHP treatment as a selective non-conventional means of starch modification. The modified features of the pressurized starches might well promote their application in drug formulation and development.

6. SUMMARY

The objective of this thesis was to investigate the applicability of three non-conventional methods - microwave processing, freeze-casting and isostatic ultrahigh pressure - as possible alternatives for pharmaceutical processing and drug formulation using potato and maize starches as model substances.

The structures and the habits of the native and the microwaved starches were studied. The effects of microwave irradiation and storage on the moisture content, adsorption behaviour and swelling properties of the polymers were investigated. The contact angles and the tensile strengths of the compacts prepared from the initial and the processed starch samples were measured and their surface free energies and polarities were calculated. Samples treated by conventional heating were used to compare the effects of microwave irradiation on the examined properties and parameters of these starches. The investigations proved that microwave irradiation and conventional heating changed the structure of the applied biopolymers irreversibly and influenced their physico-chemical properties in different ways. Volumetric heating resulted in reversible moisture loss from both types of samples. The crystallinity of potato starch was decreased, while its water retention capacity and swelling power were increased irreversibly, and its swelling capacity was increased reversibly by the thermal process applied. The corresponding parameters of maize starch were not influenced significantly by volumetric heating; this may be related to its special structure resulting in the thermal resistance of this polymer. These results allow the conclusion that for the microwave

drying of pharmaceutical formulations containing starch, the application of maize starch is advisable, with regard to the thermal resistance of this polymer, while microwave irradiation can be regarded as a suitable and selective non-conventional method for the purposeful physico-chemical modification of potato starch.

The aim of the experiments concerning the freeze-casting technique was to develop a fast-dissolving solid dosage form containing theophylline as active ingredient and potato starch as a diluent. The structure, the physical properties and mechanism of drug release from the freeze-casted units were investigated. The examined properties of the samples were compared with those of tablets compressed by an eccentric tableting machine using three different compression pressures. The freeze-casting technique proved to be an appropriate alternative for the development of porous solid drug-delivery systems. The mechanical strength of the matrices could be improved by using water-soluble additives, which stabilized the solid bodies during recrystallization upon drying. As compared with the tablets, the freeze-casted units revealed a highly porous nature and a remarkable difference in pore volume size distribution. The results demonstrated that the drug-solvent interaction, enhanced by the structural properties, resulted in a rapid delivery of the theophylline from the solid units into artificial gastric juice.

The purpose of this study was to investigate the applicability of isostatic ultra high pressure (IUHP) for the aim of drug formulation. Aqueous suspensions of potato and maize starches containing theophylline as an active pharmaceutical ingredient were subjected to IUHP. The changes in the structure and morphology of potato and maize starches were investigated. The release profile of theophylline from the pressurized samples was also studied.
The aqueous suspensions subjected to IUHP turned into highly viscous gels. The crystalline structure of maize starch was changed, while potato starch pressurized in aqueous medium retained its original X-ray pattern. The sample containing potato starch as a gel-forming polymer exhibited faster drug dissolution compared to an aqueous theophylline suspension used as a reference, while the pressurization of maize starch resulted in a gel exhibiting sustained drug release. The results of the dissolution study can be explained with the changes in structure and morphology of the starches caused by IUHP processing and with the different pressure sensitivities of the two polysaccharides.

Practical relevance of the experimental results

It is known from the literature that the energy of microwave photons is very low relative to the typical energies of chemical bonds. Hence, microwaves do not directly affect molecular structure. However, as observed in this study, moisture content has a major influence on the crystalline structure of potato starch and the water removal from this polymer is accompanied by irreversible structural changes, which result in modified physico-chemical properties. The results presented in this thesis allow the conclusion that a profound knowledge of the effects of microwave irradiation on the physico-chemical properties of frequently used excipients is essential in order to rationalize the use of dielectric heating for pharmaceutical processing. As concerns the practice of drug formulation, it can be concluded that, apart from the optimum drying parameters, adequately controlled storage conditions are also of vital importance in ensuring the appropriate moisture content of starches subjected to volumetric heating.

The freeze-casting technique and the processing by isostatic ultrahigh pressure proved to be promising new alternatives for the aim of drug formulation and design. The final product properties, which can be notably influenced by the process parameters, promote their application for specific therapeutic aims, like immediate or sustained drug delivery.

The susceptibility of the biopolymers against microwave irradiation and ultrahigh pressure strongly depended on their botanical origin, which enables a selectivity regarding the resulted effects.

As concerns the practical advantages, it should be emphasized that all non-conventional methods investigated in this work can be considered as green and mild technologies.

REFERENCES

1. Blaszczak, W., Valverde, S., Fornal, J., 2005. Effect of high pressure on the structure of potato starch, Carbohyd. Polym. 59, 377-383.

2. Cheetham, N. W. H., Tao, L., 1998. Variation in crystalline type with amylose content in maize starch granules: an X-ray powder diffraction study, Carbohyd. Polym. 36, 277-284.

3. Buléon, A., Colonna, P., Planchot, V., Ball, S., 1998. Starch granules: structure and biosynthesis, Int. J. Biol. Macromol. 23, 85-112.

4. http://www.isis.rl.ac.uk/ISIS97/donald1.jpg - starch granule structure

5. Rowe, R. C., Sheskey, P. J., Weller, P. J., 2003. Handbook of Pharmaceutical Excipients, 4th Edition, Pharmaceutical Press and American Pharmaceutical Association, pp. 603-608.

6. Swarbrick, J., Boylan, J. C., 2002. Encyclopedia of Pharmaceutical Technology, Volume 2, Marcel Dekker, New York, pp. 223-248.

7. Tomasik, P., Zaranyika, M., 1995. Nonconventional methods of modification of starch. Adv. Carbohyd. Chem. Bi. 51, 243-320.

8. http://encarta.msn.com/media_461532408/Electromagnetic_Spectrum.html

9. Acierno, D., Barba, A. A., 2004. Heat transfer phenomena during processing materials with microwave energy, Int. J. Heat Mass Tran. 40, 413-420.

10. Neas, E. D., Collins, M. J., 1998. Introduction to microwave sample preparation theory and practise. In: Kingston, H. M., Jassie, L.B. (Eds.), American Chemical Society Ch. 2, pp. 7-32.

11. Thorstenson, E. T., Chou, T-W., 1999. Microwave processing: fundamentals and applications, Compos. Part A-Appl. S. 30, 1055-1071.

12. http://www.cem.de/documents/pdf/microwave_synthesis_theory.pdf

13. Smith, B. L., Charpentier, M-H., 1993. The Microwave Engineering Handbook Volume 3, Chapman-Hall, London

14. Chen, M., Hellgeth, J. W., Ward, T. C., McGrath, J. E., 1995. Microwave processing of two phase systems: composites and polymer blends. Polym. Eng. Sci. 35 (2), 144-150.

15. Xie, Z., Yang, J., Hunag, X., Huang, Y., 1999. Microwave processing and properties of ceramics with different dielectric loss. J. European Ceramic Soc. 19, 381-387.

16. Jones, D. A., Lelyveld, S. D., Mavrofidis, S. C., Kingman, W. Q., 2002. Microwave heating applications in enviromnental engineering – a review. Res. Conservation Recycling., 34, 75-90.

17. Pan, X., Niu, G., Liu, H., 2003. Microwave-assisted extraction of tea polyphenols and tea caffeine from green tea leaves. Chem. Eng. Process. 42, 129-133.

18. Chemat, S., Ait-Amar, H., Lagha, A., Esveld, D. C., 2005. Microwave-assisted extraction of terpenes from caraway seeds. Chem. Eng. Process. 44, 1320-1326.

19. Polaert, I., Estel, L., Ledouw, A., 2005. Microwave-assisted remediation of phenol wastewater on activated charcoal. Chem. Eng. Sci. 60, 6354-6359.

20. Basak, T., Priya, A. S., 2005. Role of metallic and ceramic supports on enhanced microwave heating processes. Chem. Eng. Sci. 60, 2661-2677.

21. Li, J., Zhu, X., Zhu, J., Cheng, Z., 2007. Microwave-assisted nitroxide-mediated miniemulsion polymerization of styrene, Radiat. Phys. Chem. 23-26.

22. Seta, Y., Ghanem, A. H., Higuch, W. I., Borsadia, S., Behl, C. R., Malick, A. W., 1992. Physical model approach to understanding finite dose transport and uptake of hydrocortisone in hairless guinea-pig skin. Int. J. Pharm. 81, 89-99.

23. Genta, M. T., Villa, C., Mariani, E., Loupy, A., Petit, A., Rizetto, R., Mascarotti, A., Morini, F., Ferro, M., 2002. Microwave-assisted preparation of cyclic ketals from a cineole ketone as potential cosmetic ingredients: solvent-free synthesis, odour evaluation, in vitro cytotoxicity and antimicrobial assays. Int. J. Pharm. 231, 11-20.

24. Marcato, B., Guerra, S., Vianello, M., Scalia, S., 2003. Migration of antioxidant additives from various polyolefinic plastics into oleaginous vehicles. Int. J. Pharm. 257, 217-225.

25. Caponetti, E., Martino, D. C., Leone, M., Pedone, L., Saladino, M. L., Vetri, V., 2006. Microwave-assisted synthesis of anhydrous CdS nanoparticles in a water–oil microemulsion. J. Colloid and Interface Sci. 304, 413-418.

26. Jia, C-S., Dong, Y-W., Tu, S-J., Wang, G-W., 2007. Microwave-assisted solvent-free synthesis of substituted 2-quinolones. Tetrahedron 63, 892-897.

27. Sova, M., Babič, A., Pečar, S., Gobec, S., 2007. Microwave-assisted synthesis of hydroxyethylamine dipeptide isosteres. Tetrahedron 63, 141-147.

28. Sandoval, W. N., Arellano, F., Arnott, D., Raab, H., Vandlen, R., Lill, J. R., 2007. Rapid removal of N-linked oligosaccharides using microwave assisted enzyme catalyzed deglycosylation. Int. J. Mass Spectrom. 259, 117-123.

29. Lin, J. C., Yuan, P. M. K., Jung, D. T., 1998. Enhancement of anticancer drug delivery to the brain by microwave induced hyperthermia. Bioelectrochem. Bioenerg. 47, 259-264.

30. Droller, L. M., 2004. Multicentric study comparing intravesical chemotherapy alone and with local microwave hyperthermia for prophylaxis of recurrence of superficial transitional cell carcinoma. The Journal of Urology 172, 784.

31. Joshi, H. N., Kral, M. A., Topp, E. M., 1989. Microwave drying of aqueous tablet film coatings: a study on free films. Int. J. Pharm. 51, 19-25.

32. Sintzel, M. B., Schwach-Abdellaoui, K., Mäder, K., Stösser, R., Heller, J., Tabatabay, C., Gurny, R.,1998. Influence of irradiation sterilization on a semisolid poly(ortho ester) Int. J. Pharm. 175, 165-176.

33. Dávid, Á., Benkóczy, Z., Ács, Z., Greskovits, D., Dávid, Á. Z., 2000. The theoretical basis for scaling-up by use of the method of microwave granulation. Drug. Dev. Ind. Pharm. 26, 943-951.

34. Kapsidou, T., Nikolakakis, I., Malamataris, S., 2001. Agglomeration state and migration of drugs in wet granulations during drying. Int. J. Pharm. 227. 97-112.

35. Pan, X., Liu, H., An, Z., Wang, J., Niu, G., 2001. Microwave-enhanced dehydration and solvent washing purification of penicillin G sulfoxide. Int. J. Pharm. 220, 33-41.

36. Shahgaldian, P., Da Silva, E., Coleman, A. W., Rather, B., Zaworotko, M. J., 2003. Para-acyl-calix-arene based solid lipid nanoparticles (SLNs): a detailed study of preparation and stability parameters. Int. J. Pharm. 253, 23-38.

37. Colak, S., Korkmaz, M., 2003. Investigation of structural and dynamic features of the radicals produced in gamma irradiated sulphanilamide: an ESR study. Int. J. Pharm. 267, 49-58.

38. Sewell, G. J., Palmer, A. J., 1991. The chemical and physical stability of tree intravenous infusions subjected to frozen storage and microwave thawing. Int. J. Pharm., 72, 57-63.

39. Sewell, G. J., Palmer, A. J., Tidy, P. J., 1991. Characterization of a frozen storage-microwave thawing system for intravenous infusions. Int. J. Pharm. 70, 119-127.

40. Vromans, H., 1994. Microwave drying of pharmaceutical excipients; Comparison with conventional conductive heating, Eur. J. Pharm. Biopharm. 40 (5), 333-336.

41. McMinn, W. A. M., McLoughlin, C. M., Magee, T. R. A., 2003. Physical and dielectric properties of pharmaceutical powders. Powder Technol. 134, 40-51.

42. McMinn, W. A. M., McLoughlin, C. M., Magee, T. R. A., 2005. Microwave-convective drying characteristics of pharmaceutical powders, Powder Technol. 153, 23-33.

43. Kelen, Á., Pallai-Varsányi, E., Dávid, Á. Z., Hegedűs, Á., Pintye-Hódi, K., 2005. Select the most suitable diluent to formulate a "heat sensitive" active in case of microwave vacuum drying, Eur. J. Pharm. Sci. 25S1, S25-S27.

44. Dávid, Á. Z., Kelen, Á, Lengyel, M, Klebovich, I., Antal, I., 2005. Microwave drying and drying-kinetic study of solid pharmaceutical compounds, Eur. J. Pharm. Sci. 25S1, S77-S79.

45. Kelen, Á., Ress, S., Nagy, T., Pallai, E., Pintye-Hódi, K., 2006. Mapping of temperature distribution in pharmaceutical microwave vacuum drying, Powder Technol. 162, 133-137.

46. Kelen, A., Ress, S., Nagy, T., Pallai-Varsanyi, E., Pintye-Hodi, K., 2006. "3D layered thermography" method to map the temperature distribution of a free flowing bulk in case of microwave drying, Int. J. Heat Mass Tran. 49,1015-1021.

47. Rubinstein, M., 1987. Pharmaceutical Technology: Tableting Technology, Ellis Horwood Limited, Chichester, pp. 166-178.

48. Bajdik, J., Pintye-Hódi, K., Regdon jr., G., Erős, I., 2001. Treatment of particles with low-flow properties, Pharm. Ind. 63, 1197-1202.

49. Podczeck, F., Révész, P., 1993. Evaluation of the properties of microcrystalline and microfine cellulose powders, Int. J. Pharm. 91, 183-193.

50. Picker, K. M., 2004. Soft tableting: A new concept to tablet pressure-sensitive materials, Pharm. Dev. Techn. 9 (1), 107-121.

51. Laurie, J., Bagnall, C. M., Harris, B., Jones, R. W., Cooke, R. G., Russell-Floyd, R. S., Wang, T. H., Hammett, F. W., 1992. Colloidal suspensions for the preparation of ceramics by a freeze casting route, J. Non-Cryst. Solids, 147-148, 320-325.

52. Sofie, S. W., Dogan, F., 2001. Freeze casting of aqueous alumina slurries with glycerol, J. Am. Ceram. Soc. 84, 1459-1464.

53. Tari, G., 2003. Gelcasting ceramics: A rewiev, Am. Ceram. Soc. Bull. 82/4, 43-46.

54. Soltmann, U., Böttcher, H., Koch, D., Grathwohl, G., 2003. Freeze gelation: a new option for the production of biological ceramic composites (biocers). Mater. Lett. 57, 2861-2865.

55. Deville, S., Saiz, E., Tomsia, A. P., 2006. Freeze casting of hydroxyapatite scaffolds for bone tissue engineering, Biomaterials 27, 5480-5489.

56. Koh, Y-H., Sun, J-J., Kim, H. E., Freeze casting of porous Ni–YSZ cermets, Mater. Lett., in press (available online 24 July 2006).

57. Lee, E-J., Koh, Y-H., Yoon, B-H., Kim, H-E., Kim, H-W., 2006. Highly porous hydroxyapatite bioceramics with interconnected pore channels using camphene-based freeze casting, Mater. Lett., in press, doi:10.1016/j.matlet.2006.08.065.

58. Walther, N., Ulrich, J., 2005. Freeze casting or cold pressing – an alternative technology to form tablets. 16th International Symposium on Industrial Crystallization (ISIC) Dresden, VDI-Berichte 1901/1 343-348.

59. Donchev, D., Koch, D., Andresen, L., Ulrich, J., 2002. Freeze-casting - controlled ice crystallisation for pore design in green ceramic bodies. In J. Ulrich (ed.), BIWIC 2002, Martin-Luther-Universität, Halle-Wittenberg, Halle (Saale), pp. 237-244.

60. Donchev, D., Andresen, L., Koch, D., Ulrich, J., 2004. Einstellen einer gezielten Porosität in keramischen Grünkörpern über das kontrollierte Kristallisieren der wässrigen Phase, Chemie Ingenieur Technik 76 (11), 1688-1690.

61. Zajc, N., Obreza, A., Bele, M., Srcic, S., 2005. Physical properties and dissolution behaviour of nifedipine/mannitol solid dispersions prepared by hot melt method, Int. J. Pharm. 291, 51-58.

62. Gould, G. W., 1996. Methods for preservation and extension of shelf life. Int. J. Food Microbiol. 33, 51-64.

63. Hendrickx, M., Ludikhuyze, L., Van den Broeck, I., Weemaes, C., 1996. Effects of high pressure on enzymes related to food quality. Trends Food Sci. Tech. 9, 197-203.

64. Smelt, J. P. P. M., 1998. Recent advantages in the microbiology of high pressure processing. Trends Food Sci. Tech. 9, 152-158.

65. Perrier-Cornet, J. M., Tapin, S., Gaeta, S., Gervais, P., 2005. High-pressure inactivation of Saccharomyces cerevisiae and Lactobacillus plantarum at subzero temperatures. J. Biotechnol. 115, 405-412.

66. Torres, J. A., Velazquez, G., 2005. Commercial opportunities and research challenges in the high pressure processing of foods. J. Food Eng. 67, 95-112.

67. Chapleau, N., Ritz, M., Delépine, S., Jugiau, F., Federighi, M., de Lamballerie, M., 2006. Influence of kinetic parameters of high pressure processing on bacterial inactivation in a buffer system. Int. J. Food Microbiol. 106, 324-330.

68. http://www.abayfor.de/abayfor/_media/pdf/ZIB3/09-Meyer-Pittroff.pdf

69. Knorr D., Heinz V., Buckow R., 2006. High pressure application for food biopolymers. Biochimica et Biophysica Acta (BBA) - Proteins & Proteomics, 1764, 619-631.

70. Iucci, L., Patrignani, F., Vallicelli, M., Guerzoni, M. E., Lanciotti, R., 2007. Effects of high pressure homogenization on the activity of lysozyme and lactoferrin against Listeria monocytogenes. Food Control. 18, 558-565.

71. Considine, T., Patel, H. A., Anema, S. G., Singh, H., Creamer, L. K., 2006. Interactions of milk proteins during heat and high hydrostatic pressure treatments — A Review, Innovative Food Science & Emerging Technologies, in press, doi:10.1016/j.ifset.2006.08.003.

72. Blaszczak, W., Fornal, J, Valverde, S, Garrido, L., 2005. Pressure-induced changes in the structure of corn starches with different amylose content. Carbohyd. Polym. 61,132-140.

73. Bauer, B. A., Hartmann, M., Sommer, K., Knorr, D., 2004. Optical in situ analysis of starch granules under high pressure with a high pressure cell. Innovative Food Science and Emerging Technologies 5, 293-298.

74. Bauer, B. A., Knorr, D., 2005. The impact of pressure, temperature and treatment time on starches: pressure-induced starch gelatinisation as pressure time temperature indicator for high hydrostatic pressure processing. J. Food Eng. 68, 329-334.

75. Stute, R., Klingler, R. W., Boguslawski, S., Eshtiaghi, M. N., Knorr, D., 1996. Effects of high pressure treatment on starches. Starch/Stärke 48, 399-408.

76. Hibi, Y., Matsumoto, T., Hagiwarea, S., 1993. Effect of high pressure on the crystalline structure of various starch granules. Cereal Chem. 70, 671-676.

77. Katopo, H., Song, Y., Jane, J., 2002. Effect and mechanism of ultrahigh hydrostatic pressure on the structure and properties of starches. Carbohydr. Polym. 47, 233-244.

78. Hendrickx, M. E. G., Knorr, D., 2003. Ultra high pressure treatments of foods, Kluver Academic/Plenum Publishers, New York.

79. Fortuna, T., Juszczak, L., Palasinski, M., 1998. Change in granule porosity on modification of starch. Zywnosc. Technologia. Jakosc. 4/17, 124-130.

80. Fortuna, T., Juszczak, L., Fornal, J., 2000. Changes in some physico-chemical properties of starch granules induced by heating and microwave irradiation. Pol. J. Food. Nutr. Sci. 9/50, 17-22.

81. Brunauer, S., Emmett, P. H., Teller, E., 1938. Adsorption of gases in multimolecular layers. J. Amer. Chem. Soc. 60, 309-319.

82. Barrett, E. P., Joyner, L. G., Halenda, P. P., 1951. The determination of pore volume and area distributions in porous substances. I. Computations from nitrogen isotherms. J. Amer. Chem. Soc. 73, 373-380.

83. Juppo, A. M., 1996. Change in porosity parameters of lactose, glucose and mannitol granules caused by low compression force. Int. J. Pharm. 130, 149-157.

84. Westermarck, S., Jupo, A. M., Kervinen, L., Yliruusi, J, 1998. Pore structure and surface area of mannitol powder, granules and tablets determined with mercury porosimetry and nitrogen adsorption. Eur. J. Pharm. Biopharm. 46, 61-68.

85. Westermarck, S., 2000. Use of mercury porosimetry and nitrogen adsorption in characterisation of the pore structure of mannitol and microcrystalline cellulose powders, granules and tablets. Academic Dissertation, University of Helsinki, Phamaceutical Technology Division, pp. 2-10.

86. Fell, J. T., Newton, J. M., 1970. Determination of tablet strength by diametral-compression test. J. Pharm. Sci. 59, 688-691.

87. Owens, D. K., Wendt, R. C., 1969. Estimation of the surface free energy of polymers. J. Appl. Polym. Sci. 13, 1741-1747.

88. Herman, J., Remon, J. P., De Vilder, J., 1989. Modified starches as hydrophilic matrices for controlled oral delivery. I. Production and characterisation of thermally modified starches. Int. J. Pharm. 56, 51-63.

89. Ring, S. G., 1985. Some studies on gelation, Starch/Stärke 37, 80-87.

90. Bowen, F. E., Vadino, W. A., 1984. A simple method for differentiating sources. Drug Dev. Ind. Pharm. 10, 505-511.

91. Tsai, M. L., Li, C.F., Lii, C.Y., 1984. Effects of granular structures on the pasting behaviours of starches. Cereal Chem. 74, 750-757.

92. Li, J-Y., Yeh, A-I., 2001. Relationships between thermal, rheological characteristics and swelling power for various starches. J. Food. Eng. 50, 141-148.

93. Rolee, A., Le Meste, M., 1997. Thermomechanical behavior of concentrated starch-water preparations. Cereal. Chem. 74 (5), 581-588.

94. Dredán, J., Antal, I., Rácz, I., 1996. Evaluation of mathematical models describing drug release from lipophilic matrices. Int. J. Pharm. 145, 61-64.

95. Dredán, J., Zelkó, R., Antal, I., Bihari, E., Rácz, I., 1997. Effect of chemical properties on drug release from hydrophobic matrices. Int. J. Pharm. 160, 257-260.

96. Costa, P., Lobo, J. M. S., 2001. Modeling and comparison of dissolution profiles. Eur. J. Pharm. Sci. 13, 123-133.

97. Langenbucher, F., 1972. Linearization of dissolution rate curves by Weibull distribution. J. Pharm. Pharmacol. 24, 979-981.

98. Ritger, P. L. and Peppas, N. A., 1987. A simple equation for description of solute release II. Fickian and anomalous release from swellable devices. J. Control. Release 5, 37-42.

99. Baumgartner, S., Planinsek, O, Srcic, S., Kristl, J., 2006. Analysis of surface properties of cellulose ethers and drug release from their matrix tablets. Eur. J. Pharm. Sci. 27, 375-383.

100. Dürig, T., Fassihi, R., 2002. Guar-based monolithic matrix systems: effect of ionizable and non-ionizable substances and excipients on gel dynamics and release kinetics. J. Control. Rel. 80, 45-56.

101. Peppas, N. A., Sahlin, J. J., 1989. A simple equation for the description of solute release. III. Coupling of diffusion and relaxation. Int. J. Pharm. 57, 169-172.

102. Moore, J. W., Flanner, H. H., 1996. Mathematical comparison of dissolution profiles. Pharm. Tech. 20, 64-74.

103. Palasinski, M., Fortuna, T., Juszczak, L., Fornal, J., 2000. Changes in some physico-chemical properties of starch granules induced by heating and microwave radiation. Pol. J. Food Nutr. Sci. 9/50, 17-22.

104. Lewandowicz, G., Fornal, J., Walkowski, A., 1997. Effect of microwave radiation on physico-chemical properties and structure of potato and tapioca starches. Carbohyd. Polym. 34, 213-220.

105. Lewandowicz, G., Jankowski, T., Fornal, J., 2000. Effect of microwave radiation on physico-chemical properties and structure of cereal starches. Carbohyd. Polym. 42, 193-199.

106. Muzimbaranda, C., Tomasik, P., 1994. Microwaves in physical and chemical modification of starch, Starch/Stärke 46, 469-474.

107. Bogracheva, T. Y., Wang, Y. L., Hedley, C. L., 2001. The effect of water content on the ordered/disordered structures in starches. Biopolymers 58, 247-259.

108. Carstensen, J. T., 1993. Pharmaceutical principles of solid dosage forms, Technomic Publishing Company, Lancaster, U.S.A., pp. 183-186.

109. Stahl, P. H., 1980. Feuchtigkeit und Trocknen in der pharmazeutischen Technologie. Steinkopff Verlag, Darmstadt, pp. 51-53.

110. Sekine, M., Otobe, K., Sugiyama, J., Kawamura, Y., 2000. Effects of heating, vacuum drying and steeping on gelatinization properties and dynamic viscoelasticity of various starches. Starch/Stärke 52, 398-405.

111. Buckton, G., Darcy, P., 1999. Assessment of disorder in crystalline powders – a review of analytical techniques and their application. Int. J. Pharm. 179, 141-158.

112. Kontny, M. J., Zografi, G., 1995. Sorption of water by solids. In H. G. Brittain, Physical characterization of pharmaceutical solids, Marcel Dekker, New York, pp. 388-418.

113. Hoover, R., 2001. Composition, molecular structure and physicochemical properties of tuber and root starches: a review. Carbohyd. Polym. 45, 253-267.

114. van Oss, C. J., 1995. Hydrophobicity of biosurfaces - origin, quantitative determination and interaction energies. Colloid Surf. B. 5, 91-110.

115. Oh, E., Luner, P. E., 1999. Surface free energy of ethylcellulose films and the influence of plasticizers. Int. J. Pharm. 188, 203-219.

116. Swarbrick, J., Boylan, J. C., 2000. Encyclopedia of Pharmaceutical Technology, Volume 3. Marcel Dekker, New York, pp. 2662.

117. Walther, N., Ulrich, J., 2005. Poröse Körper durch kaltes Tablettieren, Chemie Ingenieur Technik 77, 294-297.

118. Crowley, M. M., Schroeder, B., Fredersdorf, A., Obara, S., Talarico, M., Kucera, S., McGinity, J. W., 2004. Physicochemical properties and mechanism of drug release from ethyl cellulose matrix tablets prepared by direct compression and hot-melt extrusion. Int. J. Pharm. 269, 509-552.

119. List, P. H., Muazzam, U. A., 1979. Quellung – die treibende Kraft beim Tablettenzerfall. Pharm. Ind. 41, 459-464.

120. Caramella, C., Colombo, P., Bettinetti, G., Giordano, F., Conte, U., Manna, A. L., 1984. Swelling properties of disintegrants, Acta Pharm. Technol. 30 (2), 132-139.

121. Szabó-Révész, P., Pető, K., Pintye-Hódi, K., 1986. Untersuchung der Verwandbarkeit von mikrokristallinen Cellulosen bei der Herstellung von Phenobarbital-Tabletten. Pharm. Ind. 48 (3), 289-291.

122. Pepin, X., Blanchon, S., Couarraze, G., 1999. Powder dynamic contact angle data in the pharmaceutical industry. PSST 2(3), 111-118.

ACKNOWLEDGEMENTS

Arriving to the end of my time as a Ph.D. student, I would like to take the opportunity to thank all the people and institutions who made this work possible and helped me in any way.

I would like to thank **Professor István Erős** who accepted me as a Ph.D. student in his institute and gave me the chance to work on this project.

I am particularly indebted to **Professor Piroska Szabó-Révész** my principal supervisor. Her strong enthusiasm and support in every part of this work helped me to accomplish my dissertation and achieve my educational goals during the last three years.

I am very grateful to **Professor Joachim Ulrich** for supervising my work. Over the years, he gave me the independence to work on things that interested me and encouraged it actively, thus making me feel closer to my work.

My special thanks go to **Professor Karsten Mäder** (Martin-Luther-Universität Halle-Wittenberg Institut für Pharmazeutische Technologie und Biopharmazie) and **Professor Jörg Kressler** (Martin-Luther-Universität Halle-Wittenberg Professur Physikalische Chemie der Polymere) who provided me the possibility to carry out research work in their institutes.

Working with **Dr. Zofia Funke** was an enjoyable experience. Thanks to her for supporting me with the contact angle measurements, which I enjoyed working on.
I am likewise grateful to **Christoph Blümer** for his support in performing high-pressure processing.
I thank **all of my co-authors** for their kind collaboration.
I would like to express my thanks all the nice people I met at the University of Szeged and at the Martin-Luther-University Halle-Wittenberg, who made this time very special for me.

I gratefully acknowledge the financial support from **Kultusministerium Sachsen-Anhalt**, the **German Academic Exchange Service** (DAAD) and the **Hungarian Scholarship Committee** (MÖB) and from the **Centenarium Foundation of Gedeon Richter Ltd**.

Many many thanks to **my family** and **my nearest friends** for encouraging me in my activities and for accompanying me in challenging moments.

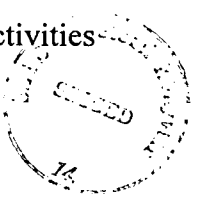

ANNEX